

Persistent coding of outcome-predictive cue features in the rat nucleus accumbens.

Authors: Jimmie M. Gmaz¹, James E. Carmichael¹, Matthijs A. A. van der Meer^{1*}

¹Department of Psychological and Brain Sciences, Dartmouth College, Hanover NH 03755

*Correspondence should be addressed to MvdM, Department of Psychological and Brain Sciences, Dartmouth College, 3 Maynard St, Hanover, NH 03755. E-mail: mvdm@dartmouth.edu.

Acknowledgments: We thank Nancy Gibson, Martin Ryan and Jean Flanagan for animal care, and Min-Ching Kuo and Alyssa Carey for technical assistance. This work was supported by Dartmouth College (Dartmouth Fellowship to JMG and JEC, and start-up funds to MvdM) and the Natural Sciences and Engineering Research Council (NSERC) of Canada (Discovery Grant award to MvdM, Canada Graduate Scholarship to JMG).

Conflict of Interest: The authors declare no competing financial interests.

1 Abstract: NOTE CURRENTLY 151 WORDS

2 The nucleus accumbens (NAc) is important for learning from feedback and for biasing and invigorating
3 behavior in response to cues that predict motivationally relevant outcomes. NAc encodes outcome-related
4 cue features such as the magnitude and identity of reward. However, little is known about how features
5 of cues themselves are encoded. We designed a decision making task where rats learned multiple sets
6 of outcome-predictive cues, and recorded single-unit activity in the NAc during performance. We found
7 that coding of cue identity and location occurred alongside coding of expected outcome, in separate and
8 overlapping populations, respectively. Furthermore, this coding persisted both during a delay period, after
9 the rat made a decision and was waiting for an outcome, and after the outcome was revealed. Encoding of
10 cue features in the NAc may enable contextual modulation of ongoing behavior, and provide an eligibility
11 trace of outcome-predictive stimuli for updating stimulus-outcome associations to inform future behavior.

12 Introduction

13 Theories of nucleus accumbens (NAc) function generally agree that this brain structure contributes to moti-
14 vated behavior, with some emphasizing a role in learning from reward prediction errors (RPEs) (Averbeck
15 & Costa 2017; Joel et al. 2002; Khamassi & Humphries 2012; Lee et al. 2012; Maia 2009; Schultz 2016; see
16 also the addiction literature on effects of drug rewards; Carelli 2010; Hyman et al. 2006; Kalivas & Volkow
17 2005), and others a role in the modulation of ongoing behavior through stimuli associated with motivation-
18 ally relevant outcomes (invigorating, directing; Floresco, 2015; Nicola, 2010; Salamone & Correa, 2012).

19 These proposals echo similar ideas on the functions of the neuromodulator dopamine (Berridge, 2012; Maia,
20 2009; Salamone & Correa, 2012; Schultz, 2016), with which the NAc is tightly linked functionally as well
21 as anatomically (Cheer et al., 2007; du Hoffmann & Nicola, 2014; Ikemoto, 2007; Takahashi et al., 2016).

22 Much of our understanding of NAc function comes from studies of how cues that predict motivationally
23 relevant outcomes (e.g. reward) influence behavior and neural activity in the NAc. Task designs that asso-
24 ciate such cues with rewarding outcomes provide a convenient access point, eliciting conditioned responses
25 such as sign-tracking and goal-tracking (Hearst & Jenkins, 1974; Robinson & Flagel, 2009), Pavlovian-
26 instrumental transfer (Estes, 1943; Rescorla & Solomon, 1967) and enhanced response vigor (Nicola, 2010;
27 Niv et al., 2007), which tend to be affected by NAc manipulations (Chang et al. 2012; Corbit & Balleine
28 2011; Flagel et al. 2011; although not always straightforwardly; Chang & Holland 2013; Giertler et al.
29 2004). Similarly, analysis of RPEs typically proceeds by establishing an association between a cue and sub-
30 sequent reward, with NAc responses transferring from outcome to the cue with learning (Day et al., 2007;
31 Roitman et al., 2005; Schultz et al., 1997; Setlow et al., 2003).

32 Surprisingly, although substantial work has been done on the coding of outcomes predicted by such cues
33 (Atallah et al., 2014; Bissonette et al., 2013; Cooch et al., 2015; Cromwell & Schultz, 2003; Day et al., 2006;
34 Goldstein et al., 2012; Hassani et al., 2001; Hollerman et al., 1998; Lansink et al., 2012; McGinty et al., 2013;
35 Nicola, 2004; Roesch et al., 2009; Roitman et al., 2005; Saddoris et al., 2011; Schultz et al., 1992; Setlow et

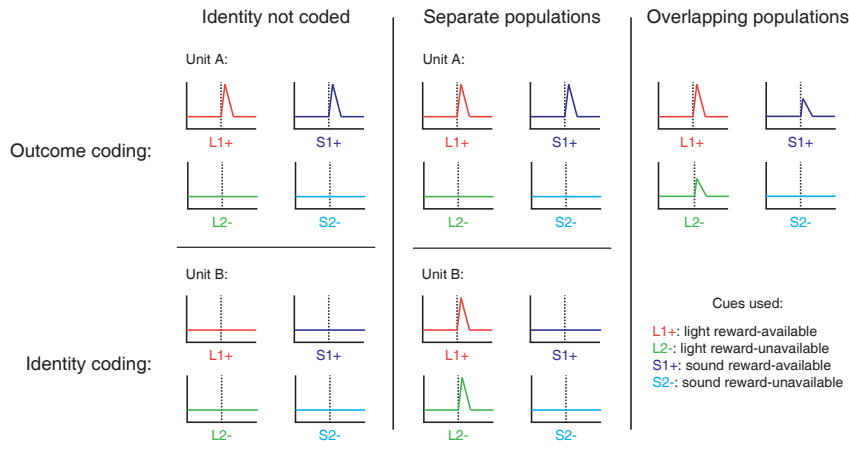
36 al., 2003; Sugam et al., 2014; West & Carelli, 2016), much less is known about how outcome-predictive cues
37 themselves are encoded in the NAc (but see; Sleezer et al., 2016). This is an important issue for at least two
38 reasons. First, in reinforcement learning, motivationally relevant outcomes are typically temporally delayed
39 relative to the cues that predict them. In order to solve the problem of assigning credit (or blame) across such
40 temporal gaps, some trace of preceding activity needs to be maintained (Lee et al., 2012; Sutton & Barto,
41 1998). For example, if you become ill after eating food X in restaurant A, depending on if you remember the
42 identity of the restaurant or the food at the time of illness, you may learn to avoid all restaurants, restaurant
43 A only, food X only, or the specific pairing of X-in-A. Therefore, a complete understanding of what is
44 learned following feedback requires understanding what trace is maintained. Since NAc is a primary target
45 of dopamine signals interpretable as RPEs, and NAc lesions impair RPEs related to timing, its activity trace
46 will help determine what can be learned when RPEs arrive (Hamid et al., 2015; Hart et al., 2014; Ikemoto,
47 2007; McDannald et al., 2011; Takahashi et al., 2016). Similarly, in a neuroeconomic framework, NAc is
48 thought to represent a domain-general subjective value signal for different offers (Bartra et al., 2013; Levy
49 & Glimcher, 2012; Peters & Büchel, 2009; Sescousse et al., 2015); having a representation of the offer itself
50 alongside this value signal would provide a potential neural substrate for updating offer value.

51 Second, for ongoing behavior, the relevance of cues typically depends on context. In experimental set-
52 tings, context may include the identity of a preceding cue, spatial or configural arrangements (Bouton, 1993;
53 Holland, 1992; Honey et al., 2014), and unsignaled rule changes, as occurs in set shifting and other cogni-
54 tive control tasks (Cohen & Servan-Schreiber, 1992; Floresco et al., 2006; Grant & Berg, 1948; Sleezer et
55 al., 2016). In such situations, the question arises how selective, context-dependent processing of outcome-
56 predictive cues is implemented. For instance, is there a gate prior to NAc such that only currently relevant
57 cues are encoded in NAc, or are all cues represented in NAc but their current values dynamically updated
58 (FitzGerald et al., 2014; Goto & Grace, 2008; Sleezer et al., 2016). Representation of cue identity would
59 allow for context-dependent mapping of outcomes predicted by specific cues.

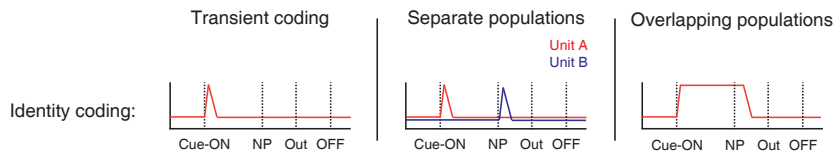
60 Thus, both from a learning and a flexible performance perspective, it is of interest to determine how cue iden-

61 tity is represented in the brain, with NAc of particular interest given its anatomical and functional position at
62 the center of motivational systems. We sought to determine whether cue identity is represented in the NAc,
63 if cue identity is represented alongside other motivationally relevant variables, such as cue outcome, and if
64 these representations are maintained after a behavioral decision has been made (see Figure 1 for a schematic
65 representation of the specific hypotheses tested). To address these questions, we recorded the activity of NAc
66 units as rats performed a task in which multiple, distinct sets of cues predicted the same outcome.

A Presence of cue identity coding



B Persistence of cue identity coding



C Quantification of coding across units and time epochs

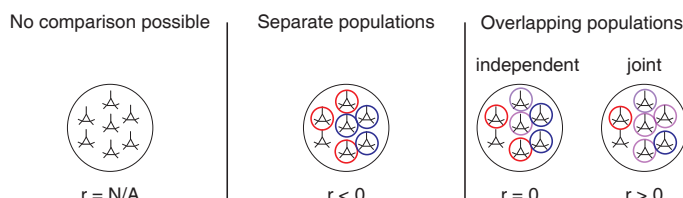


Figure 1: Schematic of hypothetical coding scenarios for cue feature coding employed by single units in the NAc across different cue features (A) and phases of a trial (B). **A:** Displayed are schematic peri-event time histograms (PETHs) illustrating putative responses to different cues under different hypotheses of how cue identity (light, sound; L, S) and outcome (reward-available, reward-unavailable; +, -) are coded. Left panel: Coding of identity is absent in the NAc. Top: Unit A encodes a motivationally relevant variable, such as expected outcome, similarly across other cue features, such as identity or physical location. Hypothetical plot is firing rate across time. L1+ (red) signifies a reward-available light cue, S1+ (navy blue) a reward-available sound cue, L2- (green) a reward-unavailable light cue, S2- (light blue) a reward-unavailable sound cue. Dashed line indicates onset of cue. Bottom: No units within the NAc discriminate their firing according to cue identity. Middle panel: Coding of identity occurs in a separate population of units from coding of other cue features such as expected outcome or physical location. Top: Same as left panel, with unit A discriminating between reward-available and reward-unavailable cues. Bottom: Unit B discriminates firing across stimulus modalities, depicted here as firing to light cues but not sound cues. Note lack of coding overlap in both units. Right panel: Coding of identity occurs in an overlapping population of cells with coding of other motivationally relevant variables. Hypothetical example demonstrating a unit that responds to reward-available cues, but firing rate is also modulated by the stimulus modality of the cue, firing most for the reward-available light cue. **B:** Displayed are schematic PETHs illustrating potential ways in which identity coding may persist over time. Left panel: Cue-onset triggers a transient response to a unit that codes for cue identity. Dashed lines indicate time of a behavioral or environmental event. 'Cue-ON' signifies cue-onset, 'NP' signifies nosepoke at a reward receptacle, 'Out' signifies when the outcome is revealed, 'OFF' signifies cue-offset. Middle and right panel: Identity coding persists at other time points, shown here during a nosepoke hold period until outcome is revealed. Coding can either be maintained by a sequence of units (middle panel) or by the same unit as during cue-onset (right panel). **C:** Schematic pool of NAc units, illustrating different analysis outcomes that discriminate between hypotheses. R values represent the correlation between sets of recoded regression coefficients (see text for analysis details). Left panel: Cue identity is not coded (A: left panel), or is only transiently represented in response to the cue (B: left panel). Middle panel: Negative correlation ($r < 0$) suggests that identity and outcome coding are represented by separate populations of units (A: middle panel), or identity coding is represented by distinct units across different points in a trial (B: middle panel). Red circles represent coding for one cue feature or point in time, blue circles for the other cue feature or point in time. Right panel: Identity and outcome coding (A: right panel), or identity coding at cue-onset and nosepoke (B: right panel) are represented by overlapping populations of units, shown here by the purple circles. The absence of a correlation ($r = 0$) suggests that the overlap of identity and outcome coding, or identity coding at cue-onset and nosepoke, is expected by chance and that the two cue features, or points in time, are coded by overlapping but independent populations from one another. A positive correlation ($r > 0$) implies a higher overlap than expected by chance, suggesting coding by a joint population. Note: The same logic applies to other aspects of the environment when the cue is presented, such as the physical location of the cue, as well as other time epochs within the task, such as when the animal receives feedback about an approach.

67 **Results**

68 **Behavior**

69 Rats were trained to discriminate between cues signaling the availability and absence of reward on a square
70 track with four identical arms for two distinct set of cues (Figure 2A). During each session, rats were pre-
71 sented sequentially with two behavioral blocks containing cues from different sensory modalities, a light and
72 a sound block, with each block containing a cue that signaled the availability of reward (reward-available),
73 and a cue that signaled the absence of reward (reward-unavailable). To maximize reward receipt, rats should
74 approach reward sites on reward-available trials, and skip reward sites on reward-unavailable trials (see Fig-
75 ure 2B for an example learning curve). All four rats learned to discriminate between the reward-available and
76 reward-unavailable cues for both the light and sound blocks as determined by reaching significance ($p < .05$)
77 on a daily chi-square test comparing approach behavior for reward-available and reward-unavailable cues for
78 each block, for at least three consecutive days (range for time to criterion: 22 - 57 days). Maintenance of
79 behavioral performance during recording sessions was assessed using linear mixed effects models for both
80 proportion of trials where the rat approached the receptacle, and trial length. Analyses revealed that the like-
81 lihood of a rat to make an approach was influenced by whether a reward-available or reward-unavailable cue
82 was presented, but was not significantly modulated by whether the rat was presented with a light or sound
83 cue (Percentage approached: light reward-available = 97%; light reward-unavailable = 34%; sound reward-
84 available = 91%; sound reward-unavailable 35%; cue identity $p = .115$; cue outcome $p < .001$; Figure 2C).
85 Thus, rats successfully discriminated the cues according to whether or not they signaled the availability of
86 reward at the reward receptacle.

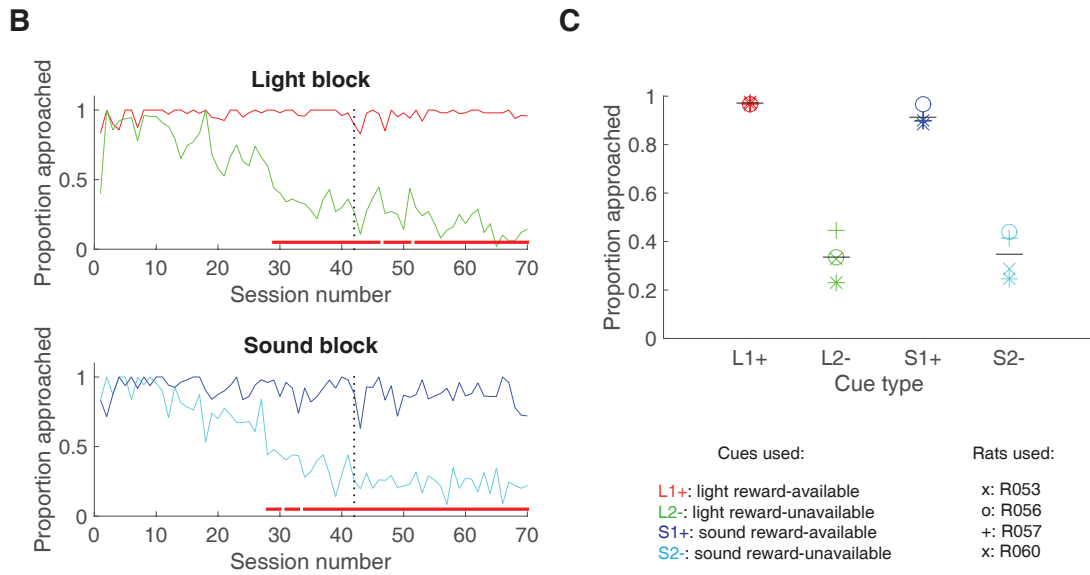
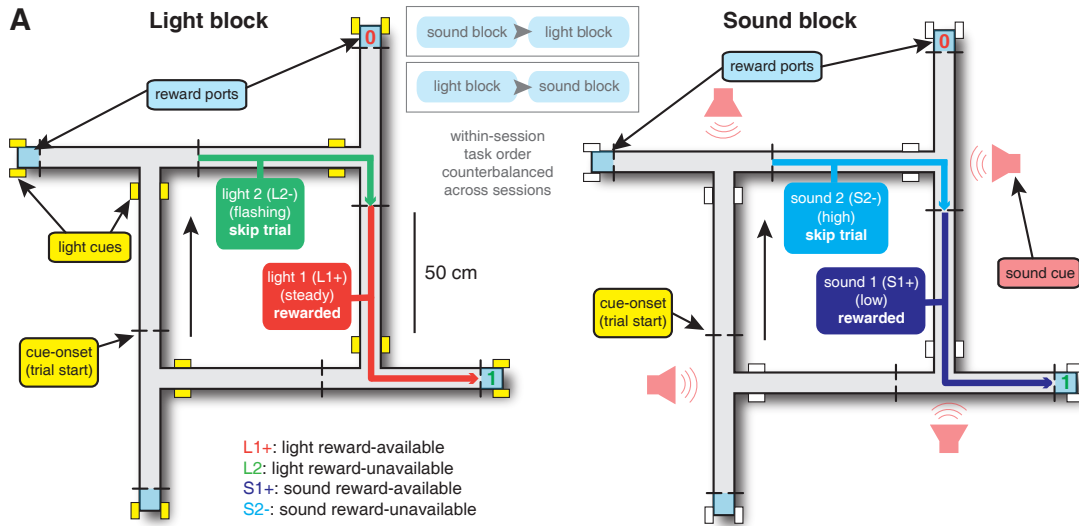


Figure 2: Schematic and performance of the behavioral task. **A:** Apparatus was a square track consisting of multiple identical T-choice points. At each choice point, the availability of 12% sucrose reward at the nearest reward receptacle (light blue fill) was signaled by one of four possible cues, presented when the rat initiated a trial by crossing a photobeam on the track (dashed lines). Photobeams at the ends of the arms by the receptacles registered nosepokes. Arrows outside of track indicate correct running direction. Left: light block showing an example trajectory for a correct reward-available (approach trial; red) and reward-unavailable (skip trial; green) trial. Rectangular boxes with yellow fill indicate location of LEDs used for light cues. Right: sound block with a correct reward-available (approach trial; navy blue) and reward-unavailable (skip trial; light blue) trial. Speakers for sound cues were placed underneath the choice points, indicated by magenta speaker icons. Ordering of the light and sound blocks was counterbalanced across sessions. Reward-available and reward-unavailable cues were presented pseudo-randomly, such that not more than two of the same type of cue could be presented in a row. Location of the cue on the track was irrelevant for behavior, all cue locations contained an equal amount of reward-available and reward-unavailable trials. **B-C:** Performance on the behavioral task. **B:** Example learning curves across sessions from a single subject (R060) showing the proportion of trials approached for reward-available (red line for light block, navy blue line for sound block) and reward-unavailable trials (green line for light block, light blue line for sound block) for light (top) and sound (bottom) blocks. Fully correct performance corresponds to an approach proportion of 1 for reward-available trials and 0 for reward-unavailable trials. Rats initially approach on both reward-available and reward-unavailable trials, and learn with experience to skip reward-unavailable trials. Red bars indicate days in which a rat statistically discriminated between reward-available and reward-unavailable cues, determined by a chi square test. Dashed line indicates time of electrode implant surgery. **C:** Proportion of trials approached for each cue, averaged across all recording sessions and shown for each rat. Different columns indicate the different cues (reward-available (red) and reward-unavailable (green) light cues, reward-available (navy blue) and reward-unavailable (light blue) sound cues). Different symbols correspond to individual subjects; horizontal black line shows the mean. All rats learned to discriminate between reward-available (~90% approached) and reward-unavailable cues (~30% approached), for both blocks (see Results for statistics).

87 **NAc encodes behaviorally relevant and irrelevant cue features**

88 We sought to address which parameters of our task were encoded by NAc activity, specifically whether the
89 NAc encodes aspects of motivationally relevant cues not directly tied to reward, such as the identity and
90 location of the cue, and whether this coding is accomplished by separate or overlapping populations (Figure
91 1A). To do this we recorded a total of 443 units with > 200 spikes in the NAc from 4 rats over 57 sessions
92 (range: 12 - 18 sessions per rat) while they performed a cue discrimination task (Table 1). Units that exhibited
93 a drift in firing rate over the course of either block, as measured by a Mann-Whitney U test comparing firing
94 rates for the first and second half of trials within a block, were excluded from further analysis, leaving
95 344 units for further analysis. The activity of 133 (39%) of these 344 units were modulated by the cue, as
96 determined by comparing 1 s pre- and post-cue activity with a Wilcoxon signed-rank test, with more showing
97 a decrease in firing ($n = 103$) than an increase ($n = 30$) around the time of cue-onset (Table 1). Within this
98 group, 24 were classified as putative fast spiking interneurons (FSIs), while 109 were classified as putative
99 medium spiny neurons (MSNs). Upon visual inspection, we observed several patterns of firing activity,
100 including units that discriminated firing upon cue-onset across various cue conditions, showed sustained
101 differences in firing across cue conditions, had transient responses to the cue, showed a ramping of activity
102 starting at cue-onset, and showed elevated activity immediately preceding cue-onset (Figure 3, supplement
103 1, supplement 2).

Task parameter	Total	\uparrow MSN	\downarrow MSN	\uparrow FSI	\downarrow FSI
All units	443	155	216	27	45
<i>Rat ID</i>					
R053	145	51	79	4	11
R056	70	12	13	17	28
R057	136	55	75	3	3
R060	92	37	49	3	3
Analyzed units	344	117	175	18	34
Cue modulated units	133	24	85	6	18
<i>GLM aligned to cue-onset</i>					
Cue identity	42 (32%)	9 (38%)	25 (29%)	0 (-)	8 (44%)
Cue location	55 (41%)	11 (46%)	33 (39%)	3 (50%)	8 (44%)
Cue outcome	26 (20%)	5 (21%)	15 (18%)	1 (17%)	5 (28%)
Approach behavior	32 (24%)	8 (33%)	19 (22%)	2 (33%)	3 (17%)
Trial length	22 (17%)	5 (21%)	14 (16%)	0 (-)	3 (17%)
Trial number	42 (32%)	11 (46%)	20 (24%)	1 (17%)	10 (56%)
Trial history	8 (6%)	1 (4%)	5 (6%)	0 (-)	1 (6%)
<i>GLM aligned to nosepoke</i>					
Cue identity	28 (21%)	3 (13%)	17 (20%)	2 (33%)	6 (33%)
Cue location	30 (23%)	2 (8%)	21 (25%)	2 (33%)	5 (28%)
Cue outcome	23 (17%)	2 (8%)	14 (16%)	1 (17%)	6 (33%)
<i>GLM aligned to outcome</i>					
Cue identity	25 (19%)	4 (17%)	15 (18%)	2 (33%)	4 (22%)
Cue location	31 (23%)	5 (21%)	23 (27%)	0 (-)	3 (17%)
Cue outcome	34 (26%)	6 (25%)	15 (18%)	4 (67%)	9 (50%)

Table 1: Overview of recorded NAc units and their relationship to task variables at various time epochs. Percentage is relative to the number of cue-modulated units (n = 133).

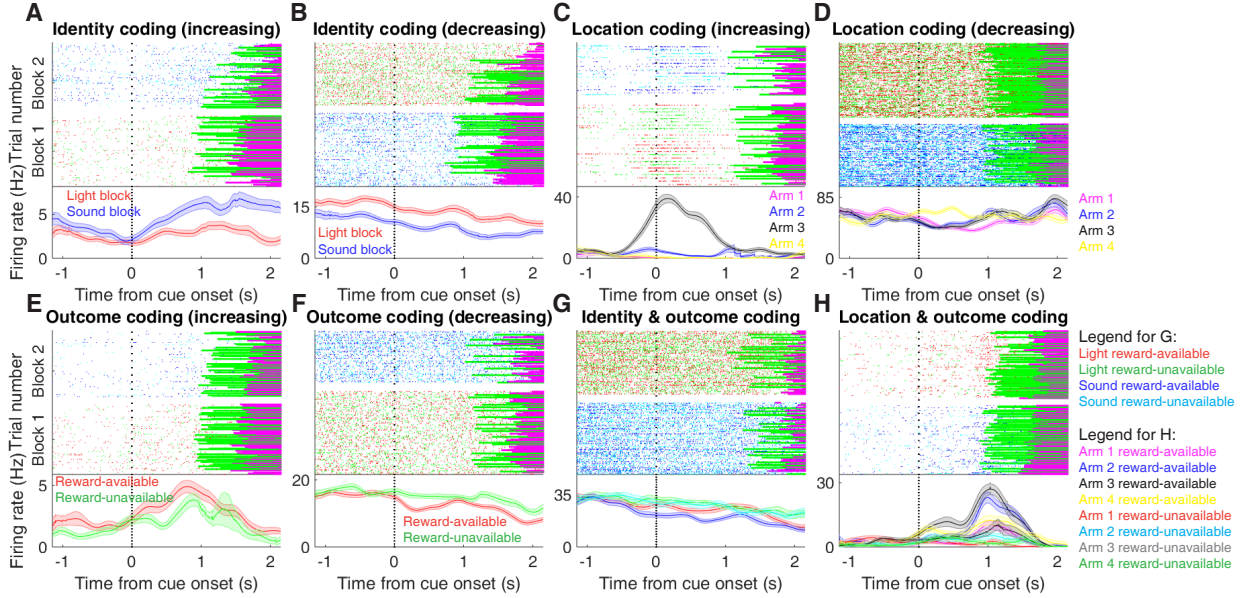


Figure 3: Examples of cue-modulated NAc units influenced by different task parameters. **A:** Example of a cue-modulated NAc unit that showed an increase in firing following the cue, and exhibited identity coding. Top: rasterplot showing the spiking activity across all trials aligned to cue-onset. Spikes across trials are color-coded according to cue type (red: reward-available light; green: reward-unavailable light; navy blue: reward-available sound; light blue: reward-unavailable sound). Green and magenta bars indicate trial termination when a rat initiated the next trial or made a nosepoke, respectively. White space halfway up the rasterplot indicates switching from one block to the next. Dashed line indicates cue-onset. Bottom: PETHs showing the average smoothed firing rate for the unit for trials during light (red) and sound (blue) blocks, aligned to cue-onset. Lightly shaded area indicates standard error of the mean. Note this unit showed a larger increase in firing to sound cues. **B:** An example of a unit that was responsive to cue identity as in A, but for a unit that showed a decrease in firing to the cue. Note the sustained higher firing rate during the light block. **C-D:** Cue-modulated units that exhibited location coding. Each color in the PETHs represents average firing response for a different cue location. **C:** The firing rate of this unit only changed on arm 3 of the task. **D:** Firing rate decreased for this unit on all arms but arm 4. **E-F:** Cue-modulated units that exhibited outcome coding, with the PETHs comparing reward-available (red) and reward-unavailable (green) trials. **E:** This unit showed a slightly higher response during presentation of reward-available cues. **F:** This unit showed a dip in firing when presented with reward-available cues. **G-H:** Examples of cue-modulated units that encoded multiple cue features. **G:** This unit showed both identity and outcome coding. **H:** An example of a unit that coded for both identity and location.

104 To characterize more formally whether these cue-modulated responses were influenced by various aspects of
105 the task, we fit a sliding window generalized linear model (GLM) to the firing rate of each cue-modulated unit
106 surrounding cue-onset, using a forward selection stepwise procedure for variable selection, a bin size of 500
107 ms for firing rate and a step size of 100 ms for the sliding window. Fitting GLMs to all trials within a session
108 revealed that a variety of task parameters accounted for a significant portion of firing rate variance in NAc
109 cue-modulated units (Figure 4A, supplement 1, supplement 2, Table 1). Notably, a significant proportion
110 of units discriminated between the light and sound block (*identity coding*: ~30% of cue-modulated units,
111 accounting for ~5% of firing rate variance) or the arms of the apparatus (*location coding*: ~40% of cue-
112 modulated units, accounting for ~4% of firing rate variance) throughout the entire window surrounding
113 cue-onset. Additionally, a substantial proportion of units discriminating between the common portion of
114 reward-available and reward-unavailable trials (*outcome coding*: ~25% of cue-modulated units, accounting
115 for ~4% of firing rate variance) was not observed until after the onset of the cue (z-score > 1.96 when
116 comparing observed proportion of units to a shuffled distribution obtained when shuffling the firing rates of
117 each unit across trials before running the GLM). Taken together, these results from the GLMs suggest that
118 the NAc encodes features of outcome-predictive cues in addition to expected outcome.

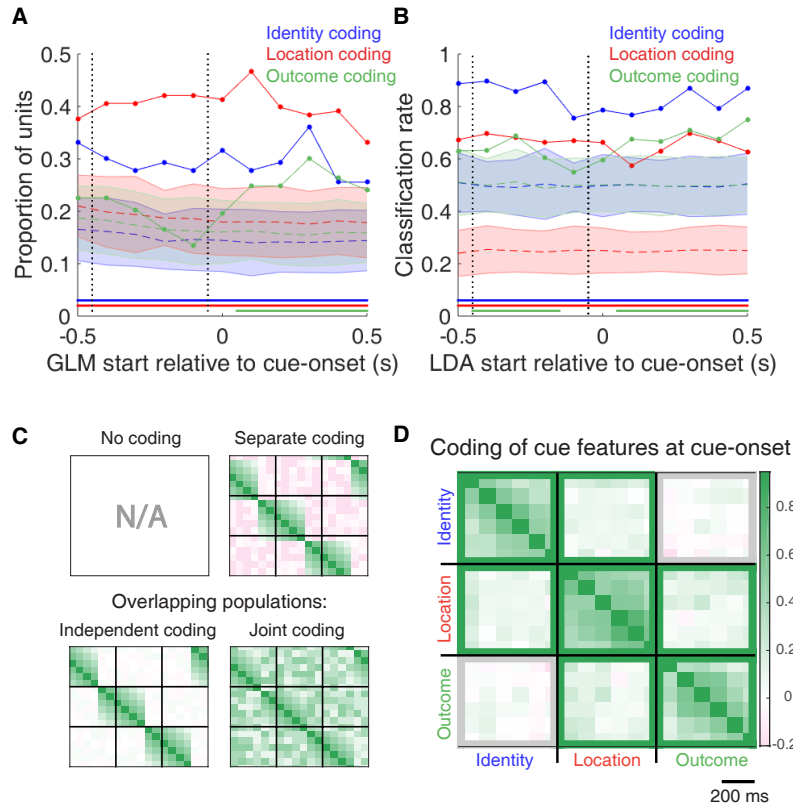


Figure 4: Summary of influence of cue features on cue-modulated NAc units at time points surrounding cue-onset. **A:** Sliding window GLM (bin size: 500 ms; step size: 100 ms) demonstrating the proportion of cue-modulated units where cue identity (blue solid line), location (red solid line), and outcome (green solid line) significantly contributed to the model at various time epochs relative to cue-onset. Dashed colored lines indicate the average of shuffling the firing rate order that went into the GLM 100 times. Error bars indicate 1.96 standard deviations from the shuffled mean. Solid lines at the bottom indicate when the proportion of units observed was greater than the shuffled distribution (z -score > 1.96). Points in between the two vertical dashed lines indicate bins where both pre- and post-cue-onset time periods were used in the GLM. **B:** Sliding window LDA (bin size: 500 ms; step size: 100 ms) demonstrating the classification rate for cue identity (blue solid line), location (red solid line), and outcome (green solid line) using a pseudoensemble consisting of the 133 cue-modulated units. Dashed colored lines indicate the average of shuffling the firing rate order that went into the cross-validated LDA 100 times. Solid lines at the bottom indicate when the classifier performance greater than the shuffled distribution (z -score > 1.96). Points in between the two vertical dashed lines indicate bins where both pre- and post-cue-onset time periods were used in the classifier. **C-D:** Correlation matrices testing the presence and overlap of cue feature coding at cue-onset. **C:** Schematic outlining the possible outcomes for coding across cue features at cue-onset, generated by correlating the recoded beta coefficients from the GLMs and comparing to a shuffled distribution (see text for analysis details). Top left: coding is not present, therefore no comparison is possible. Top right: cue features are coded by separate populations of units. Displayed is a correlation matrix with each of the 9 blocks representing correlations for two cue features across the post-cue-onset time bins from the sliding window GLM, with green representing positive correlations ($r > 0$), pink representing negative correlations ($r < 0$), and white representing no correlation ($r = 0$). X- and y-axis have the same axis labels, therefore the diagonal represents the correlation of a cue feature against itself at that particular time point ($r = 1$). Here the large amount of pink in the off-diagonal elements suggests that coding of cue features occur separately from one another. Bottom left: Coding of cue features occurs in overlapping but independent populations of units, shown here by the abundance of white and relative lack of green and pink in the off-diagonal elements. Bottom right: Coding of cue features occurs in a joint overlapping population, shown here by the large amount of green in the off-diagonal elements. **D:** Correlation matrix showing the correlation among cue identity, location, and outcome coding surrounding cue-onset. The window of GLMs used in each block is from cue-onset to the 500 ms window post-cue-onset, in 100 ms steps. Each individual value is for a sliding window GLM within that range, with the scale bar contextualizing step size. Color bar displays relationship between correlation value and color. Colored square borders around each block indicate the result of a comparison of the mean correlation of a block to a shuffled distribution, with pink indicating separate populations (z -score < -1.96), grey indicating overlapping but independent populations, and green indicating joint overlapping populations (z -score > 1.96).

119 To assess what information may be encoded at the population level, we trained a classifier on a pseudoensemble
120 of the 133 cue-modulated units (Figure 4B). Specifically, we used the firing rate of each unit for each
121 trial as an observation, and different cue conditions as trial labels (e.g. light block, sound block). A lin-
122 ear discriminant analysis (LDA) classifier with 10-fold cross-validation could correctly predict a trial above
123 chance levels for the identity and location of a cue across all time points surrounding cue-onset (z -score $>$
124 1.96 when comparing classification accuracy of data versus a shuffled distribution), whereas the ability to
125 predict whether a trial was reward-available or reward-unavailable (outcome coding) was not significantly
126 higher than the shuffled distribution for the time point containing 500 ms of pre-cue firing rate, and increased
127 gradually as a trial progressed, providing evidence that cue information is also present in the pseudoensemble
128 level.

129 To quantify the overlap of cue feature coding we correlated recoded beta coefficients from the GLMs, as-
130 signing a value of ‘1’ if a cue feature was a significant predictor for that unit and ‘0’ if not, and calculated
131 a z -score comparing the mean of the obtained correlations to the mean and standard deviation of a shuffled
132 distribution, generated by shuffling the unit ordering within an array (Figure 1A,C, 4C,D). This revealed that
133 identity was coded independently from outcome (mean $r = .009$, z -score = 0.81), and by a joint population
134 with location (mean $r = .097$, z -score = 6.61), while location and outcome were coded by a joint popula-
135 tion of units (mean $r = .119$, z -score = 8.07). Together, these findings show that various cue features are
136 represented in the NAc at both the single-unit and pseudoensemble level, with location being coded by joint
137 populations with identity and outcome, but that identity is coded independently from outcome.

138 **NAc units dynamically segment the task:**

139 Next, we sought to determine how coding of cue features evolved over time. Two main possibilities can
140 be distinguished (Figure 1B); a unit coding for a feature such as cue identity could remain persistently
141 active, or a progression of distinct units could activate in sequence. To visualize the distribution of responses
142 throughout our task space and test if this distribution is modulated by cue features, we z-scored the firing rate

143 of each unit, plotted the normalized firing rates of all units aligned to cue-onset, and sorted them according
144 to the time of peak firing rate (Figure 5). We did this separately for both the light and sound blocks, and
145 found a nearly uniform distribution of firing fields in task space that was not limited to alignment to the
146 cue (Figure 5A). Furthermore, to determine if this population level activity was similar across blocks, we
147 also organized firing during the sound blocks according to the ordering derived from the light blocks. This
148 revealed that while there was some preservation of order, the overall firing was qualitatively different across
149 the two blocks, implying that population activity distinguishes between light and sound blocks.

150 To control for the possibility that any comparison of trials would produce this effect, we divided each block
151 into two halves and looked at the correlation of the average smoothed firing rates across various combina-
152 tions of these halves across our cue-onset centered epoch to see if the across block comparisons were less
153 correlated than the within block correlations. A linear mixed effects model revealed that within block corre-
154 lations (e.g. one half of light trials vs other half of light trials) were higher and more similar than across block
155 correlations (e.g. half of light trials vs half of sound trials) suggesting that activity in the NAc discriminates
156 across light and sound blocks (mean within block correlation = .381; mean across block correlation = .342;
157 $p < .001$). This process was repeated for cue location (Figure 5B; mean within block correlation = .360;
158 mean across block correlation = .288; $p < .001$) and cue outcome (Figure 5C; mean within block correlation
159 = .345; mean across block correlation = .254; $p < .001$). Additionally, given that the majority of our units
160 showed an inhibitory response to the cue, we also plotted the firing rates according to the lowest time in fir-
161 ing, and again found some maintenance of order, but largely different ordering across the two blocks (Figure
162 5 supplement 1). Together, these results illustrate that NAc coding of task space was not confined to salient
163 events such as cue-onset, but was approximately uniformly distributed throughout the task.

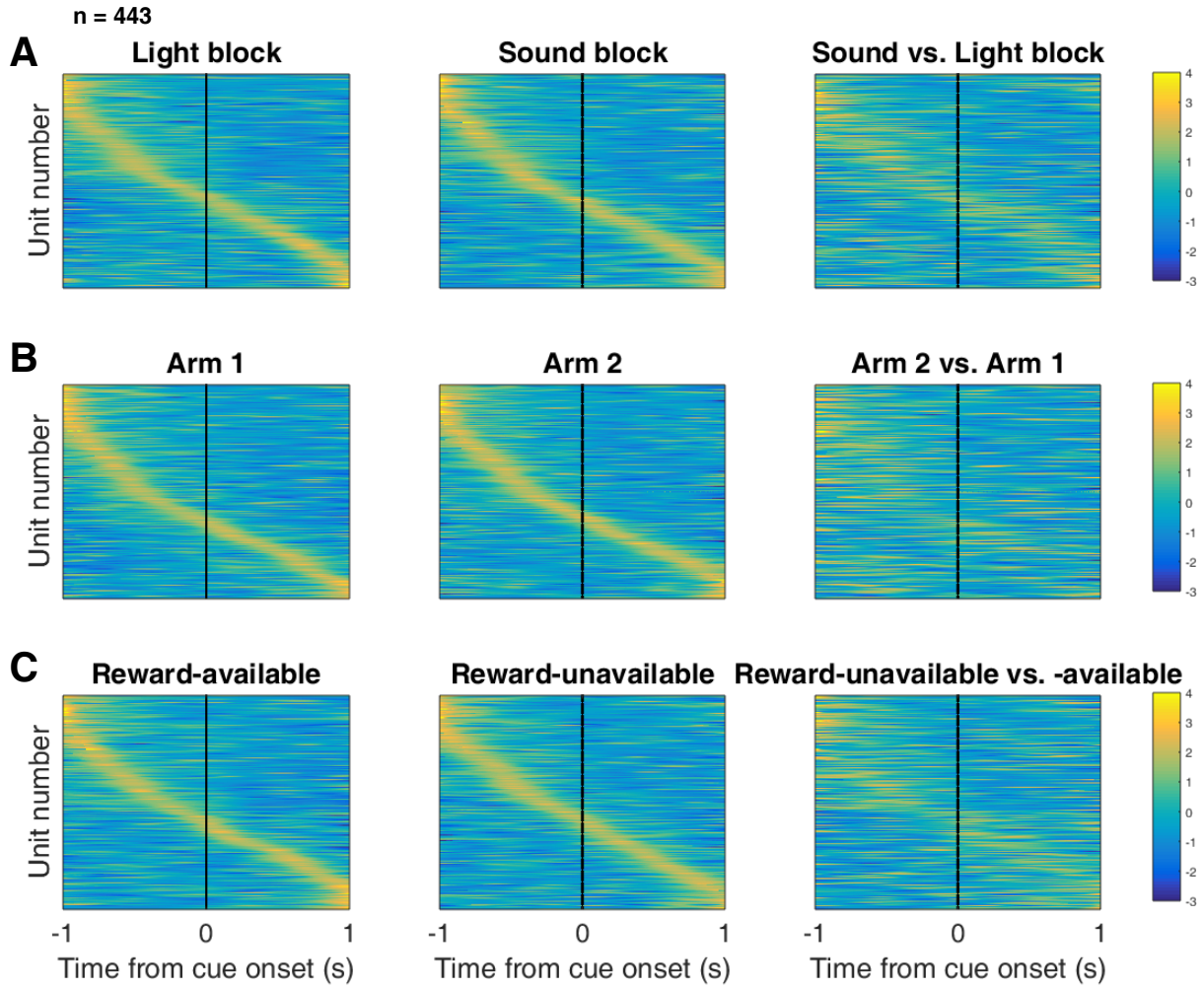


Figure 5: Distribution of NAc firing rates across time surrounding cue-onset. Each panel shows normalized (z-score) peak firing rates for all recorded NAc units (each row corresponds to one unit) as a function of time (time 0 indicates cue-onset), averaged across all trials for a specific cue type, indicated by text labels. **A**, left: Heat plot showing smoothed normalized firing activity of all recorded NAc units ordered according to the time of their peak firing rate during the light block. Each row is a units average activity across time to the light block. Dashed line indicates cue-onset. Notice the yellow band across time, indicating all aspects of visualized task space were captured by the peak firing rates of various units. **A**, middle: Same units ordered according to the time of the peak firing rate during the sound block. Note that for both blocks, units tile time approximately uniformly with a clear diagonal of elevated firing rates. **A**, right: Unit firing rates taken from the sound block, ordered according to peak firing rate taken from the light block. Note that a weaker but still discernible diagonal persists, indicating partial similarity between firing rates in the two blocks. Color bar displays relationship between z-score and color. **B**: Same layout as in **A**, except that the panels now compare two different locations on the track instead of two cue modalities. NAc units clearly discriminate between locations, but also maintain some similarity across locations, as evident from the visible diagonal in the right panel. Two example locations were used for display purposes; other location pairs showed a similar pattern. **C**: Same layout as in **A**, except that panels now compare reward-available and reward-unavailable trials. Overall, NAc units coded experience on the task, as opposed to being confined to specific task events only. Units from all sessions and animals were pooled for this analysis.

¹⁶⁴ **NAc encoding of cue features persists until outcome:**

¹⁶⁵ In order to be useful for credit assignment in reinforcement learning, a trace of the cue must be maintained
¹⁶⁶ until the outcome, so that information about the outcome can be associated with the outcome-predictive cue
¹⁶⁷ (Figure 1B). Investigation into the post-approach period during nosepoke revealed units that discriminated
¹⁶⁸ various cue features, with some units showing discriminative activity at both cue-onset and nosepoke (Figure
¹⁶⁹ 6, supplement 1, supplement 2). To quantitatively test whether representations of cue features persisted
¹⁷⁰ post-approach until the outcome was revealed, we fit sliding window GLMs to the post-approach firing
¹⁷¹ rates of cue-modulated units aligned to both the time of nosepoke into the reward receptacle, and after the
¹⁷² outcome was revealed (Figure 7A,B, supplement 1 A-D, Table 1). This analysis showed that a variety of
¹⁷³ units discriminated firing according to cue identity (~20% of cue-modulated units), location (~25% of cue-
¹⁷⁴ modulated units), and outcome (~25% of cue-modulated units), but not other task parameters, showing that
¹⁷⁵ NAc activity discriminates various cue conditions well into a trial.

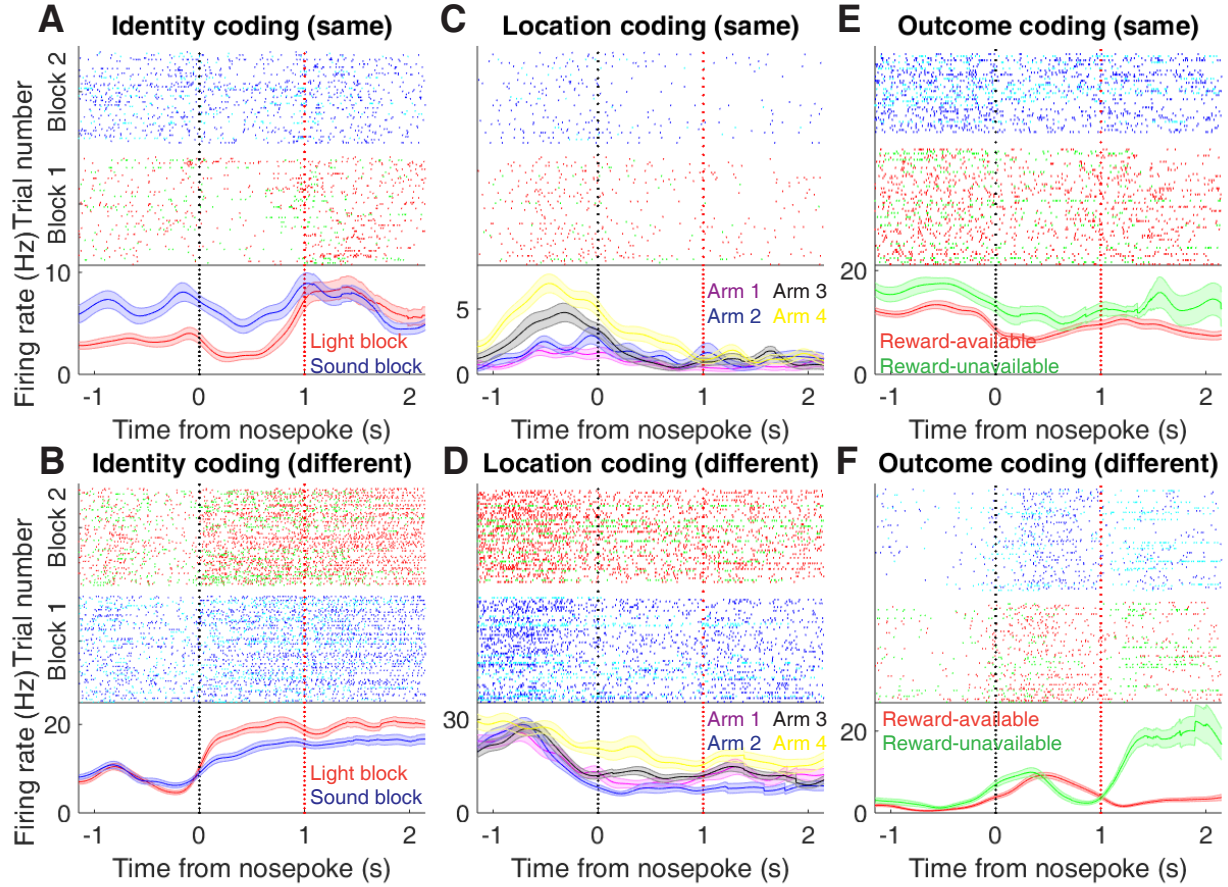


Figure 6: Examples of cue-modulated NAc units influenced by cue features at time of nosepoke. **A:** Example of a cue-modulated NAc unit that exhibited identity coding at both cue-onset and during subsequent nosepoke hold. Top: rasterplot showing the spiking activity across all trials aligned to nosepoke. Spikes across trials are color coded according to cue type (red: reward-available light; green: reward-unavailable light; navy blue: reward-available sound; light blue: reward-unavailable sound). White space halfway up the rasterplot indicates switching from one block to the next. Black dashed line indicates nosepoke. Red dashed line indicates receipt of outcome. Bottom: PETHs showing the average smoothed firing rate for the unit for trials during light (red) and sound (blue) blocks, aligned to nosepoke. Lightly shaded area indicates standard error of the mean. Note this unit showed a sustained increase in firing to sound cues during the trial. **B:** An example of a unit that was responsive to cue identity at time of nosepoke but not cue-onset. **C-D:** Cue-modulated units that exhibited location coding, at both cue-onset and nosepoke (C), and only nosepoke (D). Each color in the PETHs represents average firing response for a different cue location. **E-F:** Cue-modulated units that exhibited outcome coding, at both cue-onset and nosepoke (E), and only nosepoke (F), with the PETHs comparing reward-available (red) and reward-unavailable (green) trials.

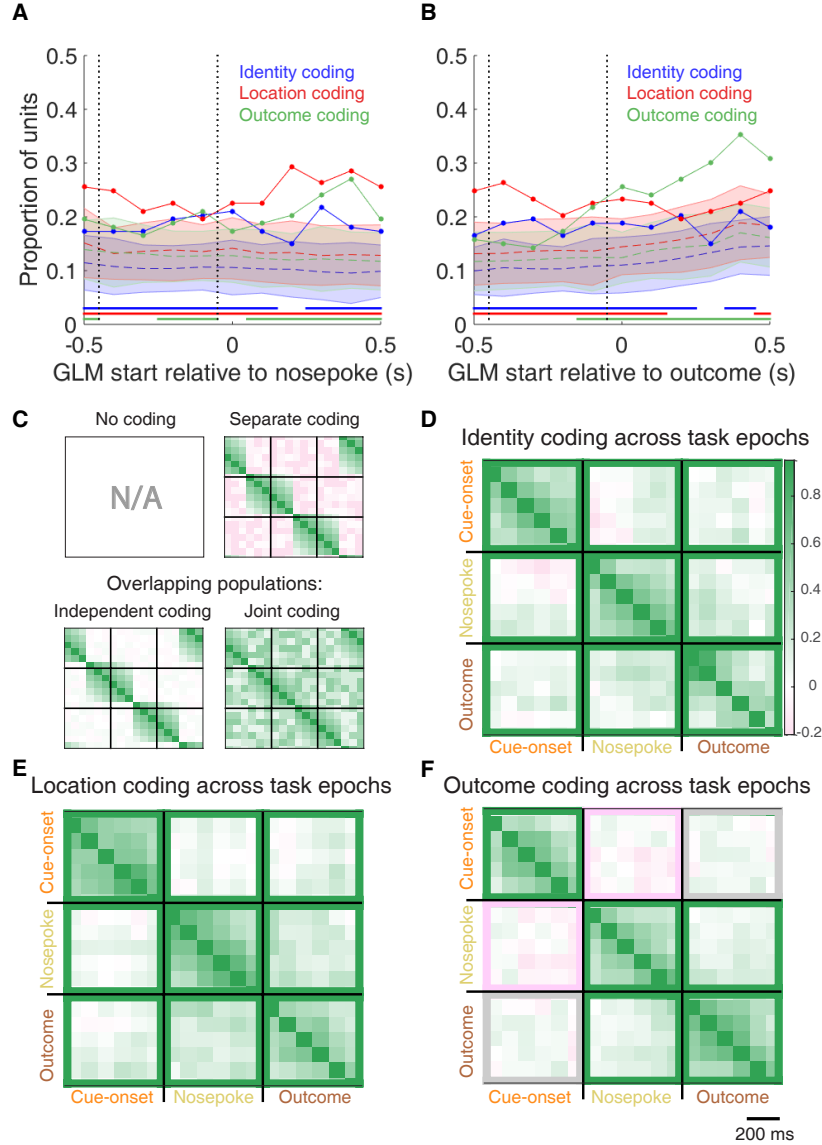


Figure 7: Summary of influence of cue features on cue-modulated NAc units at time points surrounding nosepoke and subsequent receipt of outcome. **A-B:** Sliding window GLM illustrating the proportion of cue-modulated units influenced by various predictors around time of nosepoke (A), and outcome (B). **A:** Sliding window GLM (bin size: 500 ms; step size: 100 ms) demonstrating the proportion of cue-modulated units where cue identity (blue solid line), location (red solid line), and outcome (green solid line) significantly contributed to the model at various time epochs relative to when the rat made a nosepoke. Dashed colored lines indicate the average of shuffling the firing rate order that went into the GLM 100 times. Error bars indicate 1.96 standard deviations from the shuffled mean. Solid lines at the bottom indicate when the proportion of units observed was greater than the shuffled distribution ($z\text{-score} > 1.96$). Points in between the two vertical dashed lines indicate bins where both pre- and post-cue-onset time periods were used in the GLM. **B:** Same as A, but for time epochs relative to receipt of outcome after the rat got feedback about his approach. **C-F:** Correlation matrices testing the persistence of cue feature coding across points in time.

C: Schematic outlining the possible outcomes for coding of a cue feature across various points in a trial, generated by correlating the recoded beta coefficients from the GLMs and comparing to a shuffled distribution (see text for analysis details). Top left: coding is not present, therefore no comparison is possible. Top right: a cue feature is coded by separate populations of units across time. Displayed is a correlation matrix with each of the 9 blocks representing correlations for a cue feature across time bins for two task events from the sliding window GLM, with green representing positive correlations ($r > 0$), pink negative correlations ($r < 0$), and white representing significant correlation ($r = 0$). X- and y-axis have the same axis labels, therefore the diagonal represents the correlation of cue feature against itself at that particular time point ($r = 1$). Here the large amount of pink in the off-diagonal elements suggests that coding of a cue feature is accomplished by separate populations of units across time. Bottom left: Coding of a cue feature across time occurs in overlapping but independent populations of units, shown here by the abundance of white and relative lack of green and pink in the off-diagonal elements. Bottom right: Coding of a cue feature across time occurs in a joint overlapping population, shown here by the large amount of green in the off-diagonal elements.

D: Correlation matrix showing the correlation of units that exhibited identity coding across time points after cue-onset, nosepoke, and outcome receipt. The window of GLMs used in each block is from the onset of the task phase to the 1900 ms window post-onset, in 100 ms steps. Each individual value is for a sliding window GLM within that range, with the scale bar contextualizing step size. Color bar displays relationship between correlation value and color. Colored square borders around each block indicate the result of a comparison of the mean correlation of a block to a shuffled distribution, with pink indicating separate populations ($z\text{-score} < -1.96$), grey indicating overlapping but independent populations, and green indicating joint overlapping populations ($z\text{-score} > 1.96$).

176 To determine whether NAc representations of cue features at nosepoke and outcome were encoded by a
177 similar pool of units as during cue-onset, we correlated recoded beta coefficients from the GLMs for a cue
178 feature across time points in the task, and compared the obtained correlations to correlations generated by
179 shuffling unit ordering within a recoded array (Figure 1B,C, 7C-F). This revealed that identity coding was
180 accomplished by a joint population across all three task events (cue-onset and nosepoke: mean $r = .048$, z-
181 score = 3.47; cue-onset and outcome: mean $r = .081$, z-score = 5.55; nosepoke and outcome: 10.91), while
182 joint coding was observed between nosepoke and outcome (mean $r = .147$; 3.94 standard deviations from the
183 shuffled mean). Applying this same analysis for cue location revealed a similar pattern for location coding
184 (cue-onset and nosepoke: mean $r = .058$, z-score = 4.15; cue-onset and outcome: mean $r = .093$, z-score
185 = 6.40; nosepoke and outcome: mean $r = .204$, z-score = 14.29). However, outcome coding at cue-onset
186 was separate from coding at nosepoke (mean $r = -.040$, z-score = -3.10), and independent from coding at
187 outcome (mean $r = .025$, z-score = 1.65), while joint coding was observed between nosepoke and outcome
188 (mean $r = .148$, z-score = 9.74). Together, these findings show that the NAc maintains representations of
189 cue identity and location by a joint overlapping population throughout a trial, while separate populations of
190 units encode cue outcome before and after a behavioral decision has been made.

191 To assess overlap among cue features at nosepoke and outcome receipt, we applied the same recoded coeffi-
192 cient analysis (Figure 7 supplement 1 E,F). This revealed joint coding of cue features at the time of nosepoke
193 (cue identity and location: mean $r = .124$, z-score = 8.26; cue identity and outcome: mean $r = .052$, z-score
194 = 3.65; mean $r = .097$, z-score = 6.60); while at outcome, identity was coded by a joint population with
195 both location (mean $r = .085$, z-score = 5.58), and outcome (mean $r = .039$, z-score = 2.93), and location
196 and outcome were coded by a separate population of units (mean $r = .004$, z-score = 0.28).

197 To assess the distributed coding of units for task space around outcome receipt, we aligned normalized
198 peak firing rates to nosepoke onset (Figure 7 supplement 2). This revealed a clustering of responses around
199 outcome receipt for all cue conditions where the rat would have received reward, in addition to the same
200 pattern of higher within- vs across-block correlations for cue identity (Figure 7 supplement 2 A,C; mean

201 within block correlation = .551; mean across block correlation = .484; p < .001), cue location (Figure 7
202 supplement 2 B,E; mean within block correlation = .468; mean across block correlation = .412; p < .001),
203 and cue outcome (Figure 7 supplement 2 C,F; mean within block correlation = .511; mean across block
204 correlation = .408; p < .001), further reinforcing that the NAc segments the task and represents all aspects
205 of task space.

206 Discussion

207 The main result of the present study is that NAc units encode not only the expected outcome of outcome-
208 predictive cues, but also the identity of such cues (Figure 1A). The population of units that coded for cue
209 identity was statistically independent from the population coding for expected outcome at cue-onset (i.e.
210 overlap as expected from chance), while a joint overlapping population coded for identity and outcome
211 at both nosepoke and outcome receipt (i.e. overlap greater than that expected from chance, Figure 1C).
212 Importantly, this identity coding was maintained on approach trials by a similar population of units both
213 during a delay period where the rat held a nosepoke until the outcome was received, and immediately after
214 outcome receipt (Figure 1B,C). This information was also present at the population level, with a higher than
215 chance classification accuracy for predicting the right cue condition using a pseudoensemble. Units that
216 coded different cue features (identity, outcome, location) exhibited different temporal profiles as a whole,
217 although across all recorded units a distribution of task structure was observed such that all points within
218 our analyzed task space was accounted for by the ordered peak firing rates of all units. Furthermore, this
219 distributed coding differed between various conditions with a cue feature, such as light versus sound blocks.
220 We discuss these observations and their implications below.

221 Identity coding:

222 Our finding that NAc units can discriminate between different outcome-predictive stimuli with similar moti-
223 vational significance (i.e. encodes cue identity) expands upon an extensive rodent literature examining NAc
224 correlates of conditioned stimuli (Ambroggi et al., 2008; Atallah et al., 2014; Bissonette et al., 2013; Cooch
225 et al., 2015; Day et al., 2006; Dejean et al., 2017; Goldstein et al., 2012; Ishikawa et al., 2008; Lansink et
226 al., 2012; McGinty et al., 2013; Nicola, 2004; Roesch et al., 2009; Roitman et al., 2005; Saddoris et al.,
227 2011; Setlow et al., 2003; Sugam et al., 2014; West & Carelli, 2016; Yun et al., 2004). Perhaps the most
228 comparable work in rodents comes from a study that found a subset of NAc units that modulated their firing
229 for an odor when it predicted separate but equally valued rewards (Cooch et al., 2015). The present work is
230 complementary to such *outcome identity* coding as it shows that NAc units encode *cue identity*, in addition
231 to the reward it predicts (Figure 1A). Similarly, Setlow et al. (2003) paired distinct odor cues with appetitive
232 or aversive outcomes, and found separate populations of units that encoded each cue. Furthermore, during
233 a reversal they found that the majority of units switched their selectivity, arguing that the NAc units were
234 tracking the motivational significance of these stimuli. Once again, our study was different in asking how
235 distinct cues encoding the same anticipated outcome are encoded, suggesting that the NAc dissociates their
236 representations at multiple levels of analysis (e.g. single-unit and population) even when the motivational
237 significance of these stimuli is identical. A possible interpretation of this coding of cue identity alongside
238 expected outcome is that these representations are used to associate reward with relevant features of the en-
239 vironment, so-called credit assignment in the reinforcement learning literature (Sutton & Barto, 1998). A
240 burgeoning body of human and non-human primate work has started to elucidated neural correlates of credit
241 assignment in the PFC (Akaiishi et al., 2016; Asaad et al., 2017; Chau et al., 2015; Noonan et al., 2017),
242 and given the importance of cortical inputs in NAc associative representations it is possible that information
243 related to credit assignment is relayed from the cortex to NAc (Cooch et al., 2015; Ishikawa et al., 2008).

244 Viewed within the neuroeconomic framework of decision making, functional magnetic resonance imaging
245 (fMRI) studies have found support for NAc representations of *offer value*, a domain-general common cur-
246 rency signal that enables comparison of different attributes such as reward identity, effort, and temporal
247 proximity (Bartra et al., 2013; Levy & Glimcher, 2012; Peters & Büchel, 2009; Sescousse et al., 2015). Our

248 study adds to a growing body of electrophysiological research that suggests the view of the NAc as a value
249 center, while informative and capturing major aspects of NAc processing, neglects additional contributions
250 of NAc to learning and decision making such as the offer (cue) identity signal reported here.

251 A different possible function for cue identity coding is to support contextual modulation of the motivational
252 relevance of specific cues. A context can be understood as a particular mapping between specific cues and
253 their outcomes: for instance, in context 1 cue A but not cue B is rewarded, whereas in context 2 cue B but not
254 cue A is rewarded. Successfully implementing such contextual mappings requires representation of the cue
255 identities. Indeed, Sleszer et al. (2016) recorded NAc responses during the Wisconsin Card Sorting Task, a
256 common set-shifting task used in both the laboratory and clinic, and found units that preferred firing to stimuli
257 when a certain rule, or rule category was currently active. Further support for a modulation of NAc responses
258 by strategy comes from an fMRI study that examined blood-oxygen-level dependent (BOLD) levels during
259 a set-shifting task (FitzGerald et al., 2014). In this task, participants learned two sets of stimulus-outcome
260 contingencies, a visual set and an auditory set. During testing they were presented with both simultaneously,
261 and the stimulus dimension that was relevant was periodically shifted between the two. Here, they found that
262 bilateral NAc activity reflected value representations for the currently relevant stimulus dimension, and not
263 the irrelevant stimulus. Given that BOLD activity is thought to reflect the processing of incoming and local
264 information, and not spiking output (Logothetis et al., 2001), it is possible that the relevance-gated value
265 representations observed by FitzGerald et al. (2014) are integrated with the relevant identity coding in the
266 output of the NAc, as observed in the current study.

267 Our analyses were designed to eliminate several potential alternative interpretations to cue identity coding.
268 Because the different cues were separated into different blocks, units that discriminated between cue identi-
269 ties could instead be encoding time or other slowly-changing quantities. We excluded this possible confound
270 by excluding units that showed a drift in firing between the first and second half within a block. Additionally,
271 we included time as a nuisance variable in our GLMs, to exclude firing rate variance in the remaining units
272 that could be attributed to this confound. Furthermore, we found that the temporally evolving firing rate

273 throughout a trial was more strongly correlated within a block than across blocks. However, the possibility
274 remains that instead of, or in addition to, stimulus identity, these units encode a preferred context, or even
275 a macroscale representation of progress through the session. Indeed, encoding of the current strategy could
276 be an explanation for the presence of pre-cue identity coding (Figure 4A), as well as for the differential
277 distributed coding of task structure across blocks observed in the current study (Figure 5).

278 A different potential confound is that between outcome and action value coding as the rat was only rewarded
279 for left turns. Our GLM analysis dealt with this by excluding firing rate variance accounted for by a predictor
280 that represented whether the animal approached (left turn) or skipped (right turn) the reward port at the choice
281 point, thus we were able to identify units that were modulated by the expected outcome of the cue after
282 removing variance due to action value coding. Another possible caveat is that NAc signals have been shown
283 to be modulated by response vigor (McGinty et al., 2013); to detangle this from our results we included trial
284 length (i.e. latency to arrival at the reward site) as a predictor in our GLMs, and found units with cue feature
285 correlates independent of trial length.

286 An overall limitation of the current study is that rats were never presented with both sets of cues simul-
287 taneously, and were not required to switch strategies between multiple sets of cues (this was attempted in
288 behavioral pilots, however animals took several days of training to successfully switch strategies). Addition-
289 ally, our recordings were done during performance on the well-learned behavior, and not during the initial
290 acquisition of the cue-outcome relationships when an eligibility trace would be most useful. Thus, it is
291 unknown to what extent the cue identity encoding we observed is behaviorally relevant, although extrapo-
292 lating data from other work (Sleeker et al., 2016) suggests that cue identity coding would be modulated by
293 relevance. Furthermore, NAc core lesions have been shown to impair shifting between different behavioral
294 strategies (Floresco et al., 2006), and it is possible that selectively silencing the units that prefer responding
295 for a given modality or rule would impair performance when the animal is required to use that information,
296 or artificial enhancement of those units would cause them to use the rule when it is the inappropriate strategy.

297 **Encoding of position:**

298 Our finding that cue-modulated activity was influenced by cue location supports several previous reports
299 (Lavoie & Mizumori, 1994; Mulder et al., 2005; Strait et al., 2016; Wiener et al., 2003). The NAc receives
300 inputs from the hippocampus, and the communication of place-reward information across the two structures
301 suggests that the NAc tracks locations associated with reward (Lansink et al., 2008, 2009, 2016; Pennartz,
302 2004; Sjulson et al., 2017; Tabuchi et al., 2000; van der Meer & Redish, 2011). However, it is notable
303 that in our task, location is explicitly uninformative about reward, yet coding of this uninformative variable
304 persists. The finding of distributed coding of task space is in alignment with previous studies showing that
305 NAc units can also signal progress through a sequence of cues and/or actions (Atallah et al., 2014; Berke et
306 al., 2009; Khamassi et al., 2008; Lansink et al., 2012; Mulder et al., 2004; Shidara et al., 1998), is similar
307 to observations in the basal forebrain (Tingley & Buzsáki, 2018), and may represent a temporally evolving
308 state value signal (Hamid et al., 2015; Pennartz et al., 2011). Given that the current task was pseudo-random,
309 it is possible that the rats learned the structure of sequential cue presentation, and the neural activity could
310 reflect this. However, this is unlikely as including a trial history variable in the GLM analysis did not
311 explain a significant amount of firing rate variance for the vast majority of units. In any case, NAc units
312 on the present task continued to distinguish between different locations, even though location, and progress
313 through a sequence, were explicitly irrelevant in predicting reward. We speculate that this persistent coding
314 of location in NAc may represent a bias in credit assignment, and associated tendency for rodents to associate
315 motivationally relevant events with the locations where they occur.

316 **Implications:**

317 Maladaptive decision making, as occurs in schizophrenia, addiction, Parkinson's, among others, can result
318 from dysfunctional RPE and value signals (Frank et al., 2004; Gradin et al., 2011; Maia & Frank, 2011).
319 This view has been successful in explaining both positive and negative symptoms in schizophrenia, and
320 deficits in learning from feedback in Parkinson's (Frank et al., 2004; Gradin et al., 2011). However, the

321 effects of RPE and value updating are contingent upon encoding of preceding action and cue features, the
322 eligibility trace (Lee et al., 2012; Sutton & Barto, 1998). Value updates can only be performed on these
323 aspects of preceding experience that are encoded when the update occurs. Therefore, maladaptive learning
324 and decision making can result from not only aberrant RPEs but also from altered cue feature encoding. For
325 instance, on this task the environmental stimulus that signaled the availability of reward was conveyed by two
326 distinct cues that were presented in four locations. While in our current study, the location and identity of
327 the cue did not require any adjustments in the animals behavior, we found coding of these features alongside
328 the expected outcome of the cue that could be the outcome of credit assignment computations computed
329 upstream (Akaishi et al., 2016; Asaad et al., 2017; Chau et al., 2015; Noonan et al., 2017). Identifying
330 neural coding related to an aspect of credit assignment is important as inappropriate credit assignment could
331 be a contributor to conditioned fear overgeneralization seen in disorders with pathological anxiety such as
332 generalized anxiety disorder, post-traumatic stress disorder, and obsessive-compulsive disorder (Kaczkurkin
333 et al., 2017; Kaczkurkin & Lissek, 2013; Lissek et al., 2014), and delusions observed in disorders such as
334 schizophrenia, Alzheimer's and Parkinson's (Corlett et al., 2010; Kapur, 2003). Thus, our results provide a
335 neural window into the process of credit assignment, such that the extent and specific manner in which this
336 process fails in syndromes such as schizophrenia, obsessive-compulsive disorder, etc. can be experimentally
337 accessed.

338 **Methods**

339 **Subjects:**

340 A sample size of 4 adult male Long-Evans rats (Charles River, Saint Constant, QC) from an apriori deter-
341 mined sample of 5 were used as subjects (1 rat was excluded from the data set due to poor cell yield). Rats
342 were individually housed with a 12/12-h light-dark cycle, and tested during the light cycle. Rats were food
343 deprived to 85-90% of their free feeding weight (weight at time of implantation was 440 - 470 g), and water

344 restricted 4-6 hours before testing. All experimental procedures were approved by the the University of Wa-
345 terloo Animal Care Committee (protocol# 11-06) and carried out in accordance with Canadian Council for
346 Animal Care (CCAC) guidelines.

347 **Overall timeline:**

348 Each rat was first handled for seven days during which they were exposed to the experiment room, the
349 sucrose solution used as a reinforcer, and the click of the sucrose dispenser valves. Rats were then trained
350 on the behavioral task (described in the next section) until they reached performance criterion. At this point
351 they underwent hyperdrive implantation targeted at the NAc. Rats were allowed to recover for a minimum
352 of five days before being retrained on the task, and recording began once performance returned to pre-
353 surgery levels. Upon completion of recording, animals were glosed, euthanized and recording sites were
354 histologically confirmed.

355 **Behavioral task and training:**

356 The behavioral apparatus was an elevated, square-shaped track (100 x 100 cm, track width 10 cm) containing
357 four possible reward locations at the end of track “arms” (Figure 2A). Rats initiated a *trial* by triggering a
358 photobeam located 24 cm from the start of each arm. Upon trial initiation, one of two possible light cues (L1,
359 L2), or one of two possible sound cues (S1, S2), was presented that signaled the presence (*reward-available*
360 *trial*, L1+, S1+) or absence (*reward-unavailable trial*, L2-, S2-) of a 12% sucrose water reward (0.1 mL) at
361 the upcoming reward site. A trial was classified as an *approach trial* if the rat turned left at the decision point
362 and made a nosepoke at the reward receptacle (40 cm from the decision point), while trials were classified as
363 a *skip trial* if the rat instead turned right at the decision point and triggered the photobeam to initiate the next
364 trial. A trial was labeled *correct* if the rat approached (i.e. nosepoked) on reward-available trials, and skipped
365 (i.e. did not nosepoke) on reward-unavailable trials. On reward-available trials there was a 1 second delay
366 between a nosepoke and subsequent reward delivery. *Trial length* was determined by measuring the length

367 of time from cue-onset until nosepoke (for approach trials), or from cue-onset until the start of the following
368 trial (for skip trials). Trials could only be initiated through clockwise progression through the series of arms,
369 and each entry into the subsequent arm on the track counted as a trial. Cues were present until 1 second after
370 outcome receipt on approach trials, and until initiating the following trial on skip trials.

371 Each session consisted of both a *light block* and a *sound block* with 100 trials each. Within a block, one cue
372 signaled reward was available on that trial (L1+ or S1+), while the other signaled reward was not available
373 (L2- or S2-). Light block cues were a flashing white light, and a steady yellow light. Sound block cues
374 were a 2 kHz sine wave (low) and a 8 kHz sine wave (high) whose amplitude was modulated from 0 to
375 maximum by a 2 Hz sine wave. Outcome-cue associations were counterbalanced across rats, e.g. for some
376 rats L1+ was the flashing white light, and for others L1+ was the steady yellow light. The order of cue
377 presentation was pseudorandomized so that the same cue could not be presented more than twice in a row.
378 Block order within each day was also pseudorandomized, such that the rat could not begin a session with
379 the same block for more than two days in a row. Each session consisted of a 5 minute pre-session period
380 on a pedestal (a terracotta planter filled with towels), followed by the first block, then the second block,
381 then a 5 minute post-session period on the pedestal. For approximately the first week of training, rats were
382 restricted to running in the clockwise direction by presenting a physical barrier to running counterclockwise.
383 Cues signaling the availability and unavailability of reward, as described above, were present from the start
384 of training. Rats were trained for 200 trials per day (100 trials per block) until they discriminated between
385 the reward-available and reward-unavailable cues for both light and sound blocks for three consecutive days,
386 according to a chi-square test rejecting the null hypothesis of equal approaches for reward-available and
387 reward-unavailable trials, at which point they underwent electrode implant surgery.

388 **Surgery:**

389 Surgical procedures were as described previously (Malhotra et al., 2015). Briefly, animals were administered
390 analgesics and antibiotics, anesthetized with isoflurane, induced with 5% in medical grade oxygen and main-

tained at 2% throughout the surgery (~ 0.8 L/min). Rats were then chronically implanted with a “hyperdrive” consisting of 20 independently drivable tetrodes, with 4 designated as references tetrodes, and the remaining 16 either all targeted for the right NAc (AP +1.4 mm and ML +1.6 mm relative to bregma; Paxinos & Watson 1998), or 12 in the right NAc and 4 targeted at the mPFC (AP +3.0 mm and ML +0.6 mm, relative to bregma; only data from NAc tetrodes was analyzed). Following surgery, all animals were given at least five days to recover while receiving post-operative care, and tetrodes were lowered to the target (DV -6.0 mm) before being reintroduced to the behavioral task.

398 Data acquisition and preprocessing:

399 After recovery, rats were placed back on the task for recording. NAc signals were acquired at 20 kHz with a
400 RHA2132 v0810 preamplifier (Intan) and a KJE-1001/KJD-1000 data acquisition system (Amplipex). Signals
401 were referenced against a tetrode placed in the corpus callosum above the NAc. Candidate spikes for
402 sorting into putative single units were obtained by band-pass filtering the data between 600-9000 Hz, thresh-
403 olding and aligning the peaks (UltraMegaSort2k, Hill et al., 2011). Spike waveforms were then clustered
404 with KlustaKwik using energy and the first derivative of energy as features, and manually sorted into units
405 (MClust 3.5, A.D. Redish et al., <http://redishlab.neuroscience.umn.edu/MClust/MClust.html>). Isolated units
406 containing a minimum of 200 spikes within a session were included for subsequent analysis. Units were
407 classified as FSIs by an absence of interspike intervals (ISIs) > 2 s, while MSNs had a combination of ISIs
408 > 2 s and phasic activity with shorter ISIs (Atallah et al., 2014; Barnes et al., 2005).

409 Data analysis:

410 *Behavior.* To determine if rats distinguished behaviorally between the reward-available and reward-unavailable
411 cues (*cue outcome*), we generated linear mixed effects models to investigate the relationships between cue
412 type and the proportion of trials approached, with *cue outcome* (reward available or not) and *cue identity*
413 (light or sound) as fixed effects, and the addition of an intercept for rat identity as a random effect. For each

414 cue, the average proportion of trials approached for a session was used as the response variable. Contribu-
415 tion of cue outcome to behavior was determined by comparing the full model to a model with cue outcome
416 removed.

417 *Neural data.* Given that some of our analyses compare firing rates across time, particularly comparisons
418 across blocks, we sought to exclude units with unstable firing rates that would generate spurious results
419 reflecting a drift in firing rate over time unrelated to our task. We used a multipronged strategy to address this
420 potential confound. As a first step, we ran a Mann-Whitney U test comparing the cue-modulated firing rates
421 for the first and second half of trials within a block, and excluded 99 of 443 units from analysis that showed
422 a significant change for either block, leaving 344 units for further analyses by our GLM. Furthermore, we
423 included time (trial number) as a nuisance variable in our GLMs to control for firing rate variance account
424 for by this confound (see below). To investigate the contribution of different cue features (*cue identity*, *cue*
425 *location* and *cue outcome*) on the firing rates of NAc single units, we first determined whether firing rates for
426 a unit were modulated by the onset of a cue by collapsing across all cues and comparing the firing rates for the
427 1 s preceding cue-onset with the 1 s following cue-onset. Single units were considered to be *cue-modulated*
428 if a Wilcoxon signed-rank test comparing pre- and post-cue firing was significant at $p < .01$. Cue-modulated
429 units were then classified as either increasing or decreasing if the post-cue activity was higher or lower than
430 the pre-cue activity, respectively.

431 To determine the relative contribution of different task parameters to firing rate variance (as in Figure 4A,
432 supplement 1), a forward selection stepwise GLM using a Poisson distribution for the response variable was
433 fit to each cue-modulated unit, using data from every trial in a session. Cue identity (light block, sound
434 block), cue location (arm 1, arm 2, arm 3, arm 4), cue outcome (reward-available, reward-unavailable),
435 behavior (approach, skip), trial length, trial number, and trial history (reward availability on the previous 2
436 trials) were used as predictors, with firing rate as the response variable. The GLMs were fit using a 500 ms
437 sliding window moving in 100 ms steps centered at 250 ms pre-cue (so no post-cue activity was included)
438 to centered at 750 ms post-cue, such that 11 different GLMs were fit for each unit, tracking the temporal

439 dynamics of the influence of task parameters on firing rate around the onset of the cue. Units were classified
440 as being modulated by a given task parameter if addition of the parameter significantly improved model fit
441 using deviance as the criterion ($p < .01$), and the total proportion of cue-modulated units influenced by a
442 task parameter was counted for each time bin. A comparison of the R-squared value between the final model
443 and the final model minus the predictor of interest was used to determine the amount of firing rate variance
444 explained by the addition of that predictor for a given unit. To control for the amount of units that would
445 be affected by a predictor by chance, we shuffled the trial order of firing rates for a particular unit within
446 a time bin, ran the GLM with the shuffled firing rates, counted the proportion of units encoding a predictor,
447 and took the average of this value over 100 shuffles. We then calculated how many z-scores the observed
448 proportion was from the mean of the shuffled distribution. For this and all subsequent shuffle analyses, we
449 used a z-score of greater than 1.96 or less than -1.96 as a marker of significance.

450 To get a sense of the predictive power of these cue feature representations we trained a classifier using firing
451 rates from a pseudoensemble comprised of our 133 cue-modulated units (Figure 4B). We created a matrix
452 of firing rates for each time epoch surrounding cue-onset where each row was an observation representing
453 the firing rate for a trial, and each column was a variable representing the firing rate for a given unit. Trial
454 labels, or classes, were each condition for a cue feature (e.g. light and sound for cue identity), making sure
455 to align trial labels across units. We then ran LDA on these matrices, using 10-fold cross validation to train
456 the classifier on 90% of the trials and testing its predictions on the held out 10% of trials, and repeated this
457 approach to get the classification accuracy for 100 iterations. To test if the classification accuracy was greater
458 by chance, we shuffled the order of firing rates for each unit before we trained the classifier. We repeated
459 this for 100 shuffled matrices for each time point, and calculated how many z-scores the mean classification
460 rate of the observed data was from the mean of the shuffled distribution.

461 To determine the degree to which coding of cue identity, cue location, and cue outcome overlapped within
462 units we correlated the recoded beta coefficients from the GLMs for the cue features (Figure 4C,D). Specifi-
463 cally, we generated an array for each cue feature at each point in time where for all cue-modulated units we

464 coded a ‘1’ if the cue feature was a significant predictor in the final model, and ‘0’ if it was not. We then
465 correlated an array of the coded 0s and 1s for one cue feature with a similar array for another cue feature, re-
466 peating this process for all post cue-onset sliding window combinations. The NAc was determined as coding
467 a pair of cue features in a) separate populations of units if there was a significant negative correlation ($r <$
468 0), b) an independently coded overlapping population of units if there was no significant correlation ($r = 0$),
469 or c) a jointly coded overlapping population of units if there was a significant positive correlation ($r > 0$).
470 To summarize the correlation matrices generated from this analysis, we shuffled the unit ordering for each
471 array 100 times, took the mean of the 36 correlations for a block comparison for each of the 100 shuffles
472 for an analysis window, and used the mean and standard deviation of these shuffled correlation averages to
473 compare to the mean of the comparison block for the actual data.

474 To better visualize responses to cues and enable subsequent population level analyses (as in Figures 3, 5),
475 spike trains were convolved with a Gaussian kernel ($\sigma = 100$ ms), and peri-event time histograms (PETHs)
476 were generated by taking the average of the convolved spike trains across all trials for a given task condition.
477 To visualize NAc representations of task space within cue conditions, normalized spike trains for all units
478 were ordered by the location of their maximum or minimum firing rate for a specified cue condition (Figure
479 5). To compare representations of task space across cue conditions for a cue feature, the ordering of units
480 derived for one condition (e.g. light block) was then applied to the normalized spike trains for the other
481 condition (e.g. sound block). To assess whether the task distributions were different across cue conditions,
482 we split each cue condition into two halves, controlling for the effects of time by shuffling trial ordering
483 before the split, and calculated the correlation of the temporally evolving smoothed firing rate across each of
484 these halves, giving us 6 correlation values for each unit. We then concatenated these 6 values across all 443
485 units to give us an array of 2658 correlation coefficients. We then fit a linear mixed effects model, trying to
486 predict these block comparison correlations with comparison type (e.g. 1st half of light block vs. 1st half of
487 sound sound) as a fixed-effect term, and unit number as a random-effect term. Comparison type is nominal,
488 so dummy variables were created for the various levels of comparison type, and coefficients were generated
489 for each condition, referenced against one of the within-within comparison types (e.g. 1st half of light block

490 vs. 2nd half of light block). The NAc was considered to discriminate across cue conditions if across-block
491 correlations were lower than within-block correlations. Additionally, we ran a model comparison between
492 the above model and a null model with just unit number, to see if adding comparison type improved model
493 fit.

494 To identify the responsivity of units to different cue features at the time of nosepoke into a reward receptacle,
495 and subsequent reward delivery, the same cue-modulated units from the cue-onset analyses were analyzed at
496 the time of nosepoke and outcome receipt using identical analysis techniques for all approach trials (Figures
497 6, 7). To compare whether coding of a given cue feature was accomplished by the same or distinct population
498 of units across time epochs, we ran the recoded coefficient correlation that was used to assess the degree of
499 overlap among cue features within a time epoch. All analyses were completed in MATLAB R2015a, the
500 code is available on our public GitHub repository (<http://github.com/vandermeerlab/papers>), and the data
501 can be accessed through DataLad.

502 **Histology:**

503 Upon completion of the experiment, recording channels were glosed by passing $10 \mu A$ current for 10 sec-
504 onds and waiting 5 days before euthanasia, except for rat R057 whose implant detached prematurely. Rats
505 were anesthetized with 5% isoflurane, then asphyxiated with carbon dioxide. Transcardial perfusions were
506 performed, and brains were fixed and removed. Brains were sliced in $50 \mu m$ coronal sections and stained
507 with thionin. Slices were visualized under light microscopy, tetrode placement was determined, and elec-
508 trodes with recording locations in the NAc were analyzed (Figure 8).

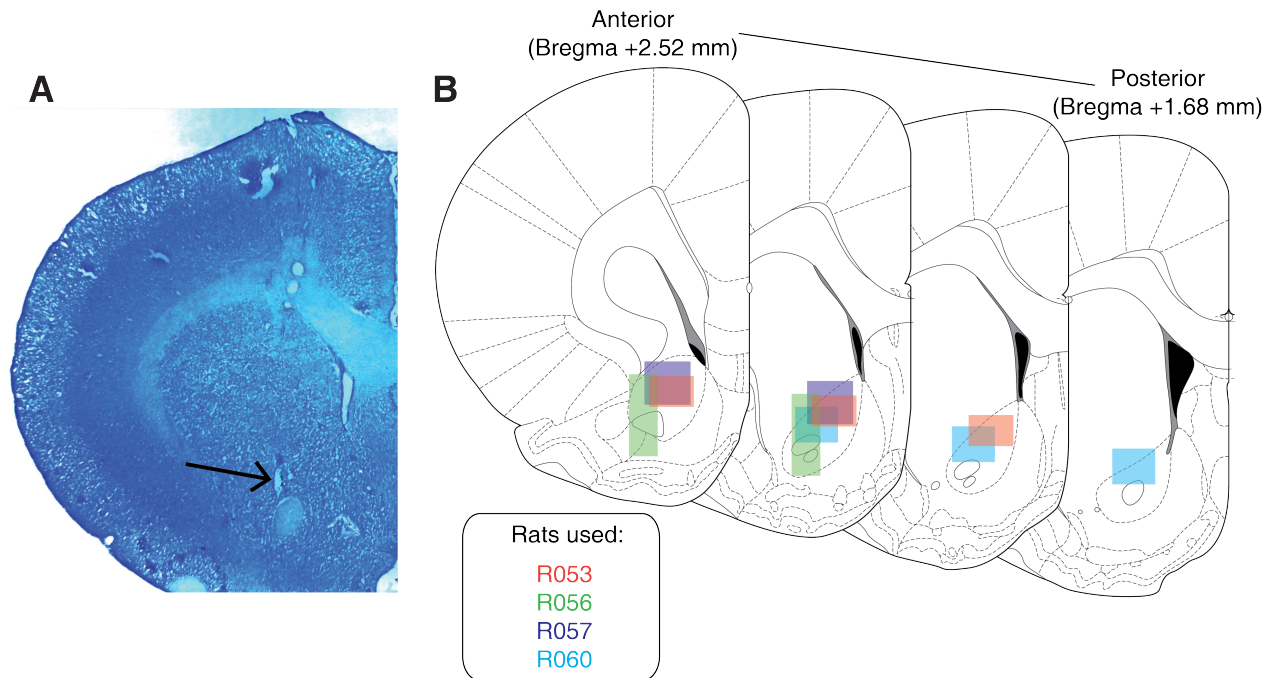


Figure 8: Histological verification of recording sites. Upon completion of experiments, brains were sectioned and tetrode placement was confirmed. **A:** Example section from R060 showing a recording site in the NAc core just dorsal to the anterior commissure (arrow). **B:** Schematic showing recording areas for all subjects.

509 **Figure supplements**

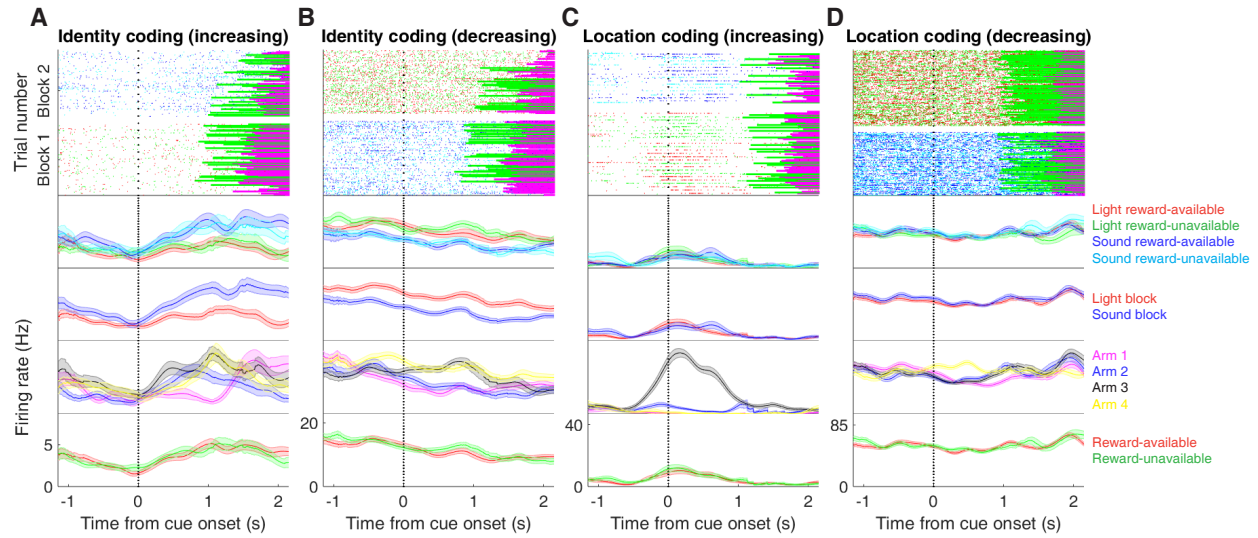


Figure 3 supplement 1: Expanded examples of cue-modulated NAc units influenced by different task parameters for Figure 3A-D, showing firing rate breakdown by: cue type (top PETH), cue identity (top-middle PETH), cue location (bottom-middle PETH), and cue outcome (bottom PETH).

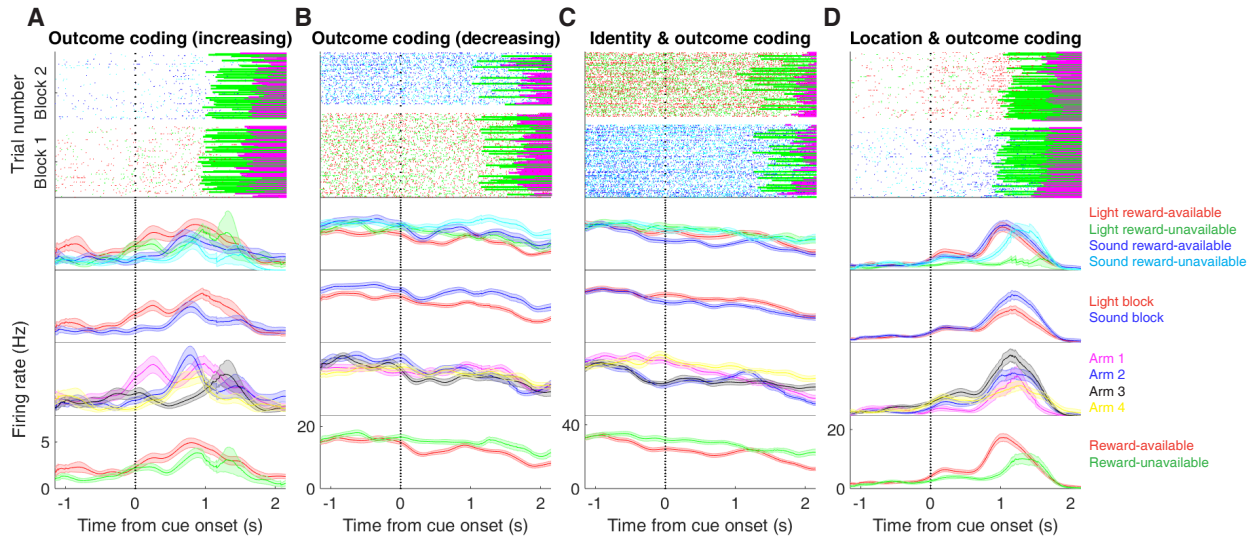


Figure 3 supplement 2: Expanded examples of cue-modulated NAc units influenced by different task parameters for Figure 3E-H, showing firing rate breakdown by: cue type (top PETH), cue identity (top-middle PETH), cue location (bottom-middle PETH), and cue outcome (bottom PETH).

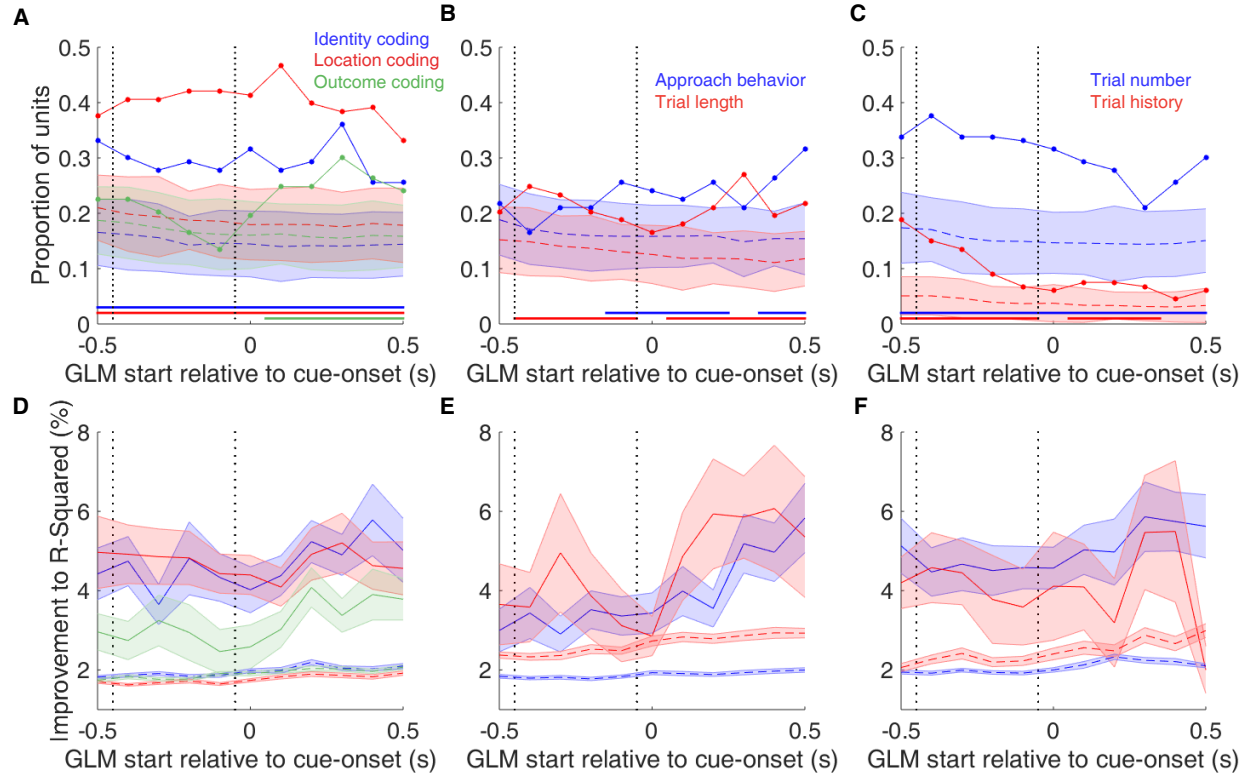


Figure 4 supplement 1: Summary of influence of various task parameters on cue-modulated NAc units at time points surrounding cue-onset. **A-C:** Sliding window GLM illustrating the proportion of cue-modulated units influenced by various predictors around time of cue-onset. **A:** Sliding window GLM (bin size: 500 ms; step size: 100 ms) demonstrating the proportion of cue-modulated units where cue identity (blue solid line), location (red solid line), and outcome (green solid line) significantly contributed to the model at various time epochs relative to cue-onset. Dashed colored lines indicate the average of shuffling the firing rate order that went into the GLM 100 times. Error bars indicate 1.96 standard deviations from the shuffled mean. Solid lines at the bottom indicate when the proportion of units observed was greater than the shuffled distribution (z -score > 1.96). Points in between the two vertical dashed lines indicate bins where both pre- and post-cue-onset time periods were used in the GLM. **B:** Same as A, but for approach behavior and trial length. **C:** Same as A, but for trial number and trial history. **D-F:** Average improvement to model fit. **D:** Average percent improvement to R^2 for units where cue identity, location, or outcome were significant contributors to the final model for time epochs surrounding cue-onset. Shaded area around mean represents the standard error of the mean. **E:** Same as D, but for approach behavior and trial length. **F:** Same D, but for trial number and trial history.

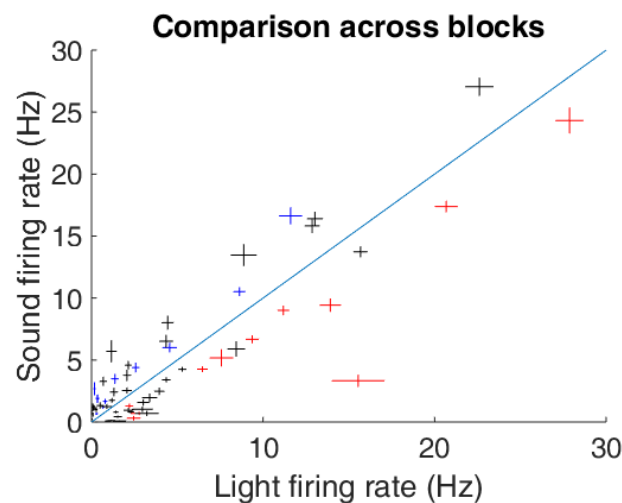


Figure 4 supplement 2: Scatter plot depicting comparison of firing rates for cue-modulated units across light and sound blocks. Crosses are centered on the mean firing rate, range represents the standard error of the mean. Colored crosses represents units that had cue identity as a significant predictor of firing rate variance in the GLM centered at cue-onset (blue are sound block preferring, red are light block preferring), whereas black crosses represent units where cue identity was not a significant predictor of firing rate variance. Diagonal dashed line indicates point of equal firing across blocks.

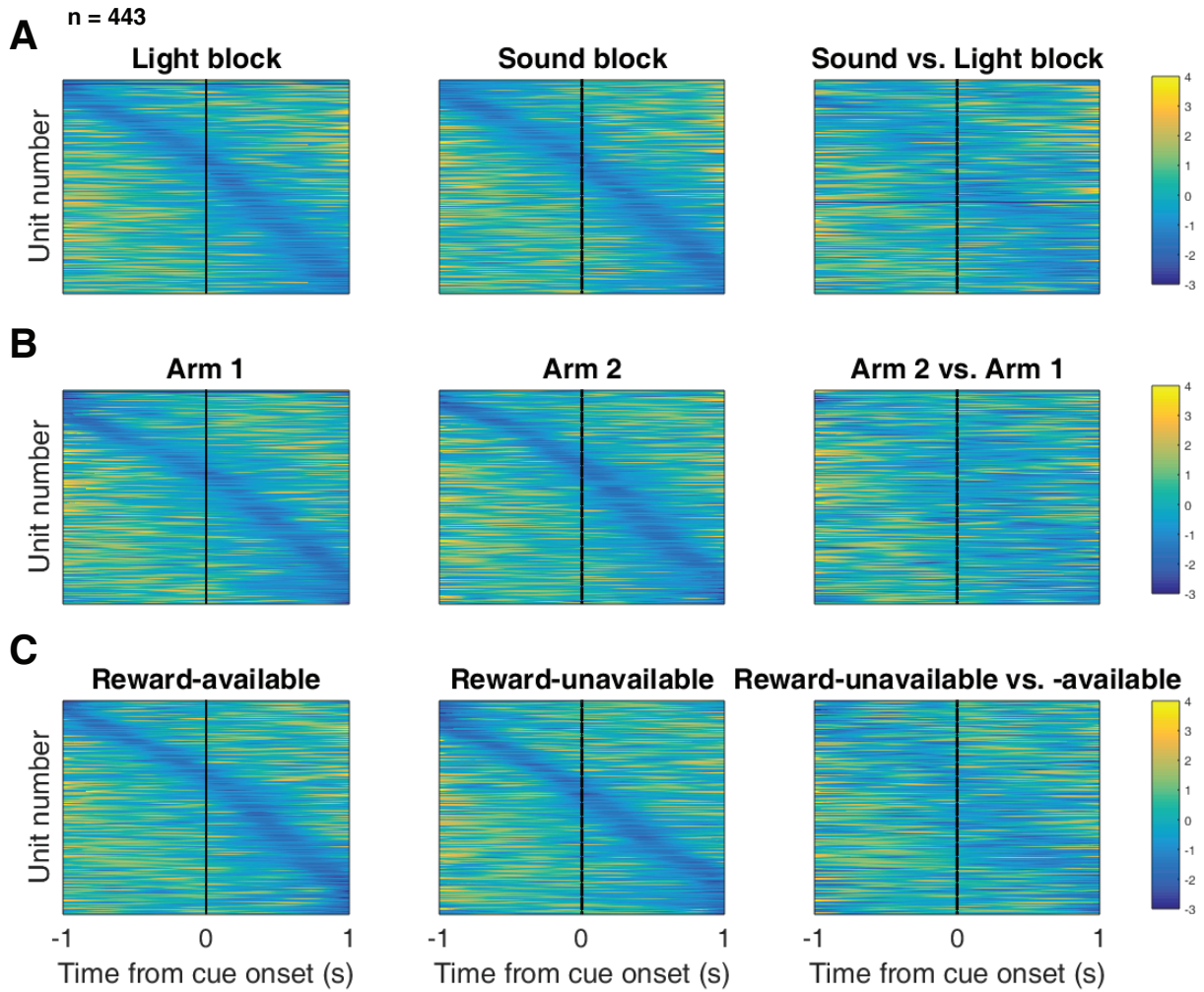


Figure 5 supplement 1: Distribution of NAc firing rates across time surrounding cue-onset. Each panel shows normalized (z-score) minimum firing rates for all recorded NAc units (each row corresponds to one unit) as a function of time (time 0 indicates cue-onset), averaged across all trials for a specific cue type, indicated by text labels. **A:** Responses during different stimulus blocks as in Figure 5A, but with units ordered according to the time of their minimum firing rate. **B:** Responses during trials on different arms as in Figure 5B, but with units ordered by their minimum firing rate. **C:** Responses during cues signaling different outcomes as in Figure 5C, but with units ordered by their minimum firing rate. Overall, NAc units coded experience on the task, as opposed to being confined to specific task events only. Units from all sessions and animals were pooled for this analysis.

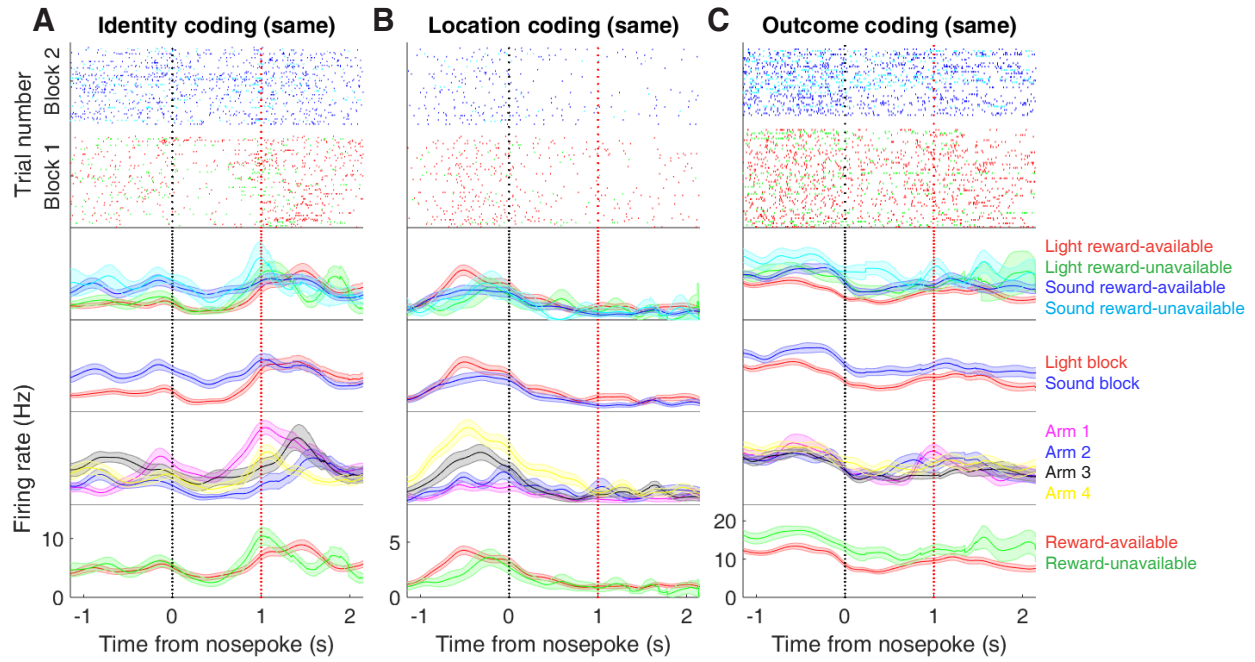


Figure 6 supplement 1: Expanded examples of cue-modulated NAc units influenced by different cue features at both cue-onset and during subsequent nosepoke hold for Figure 6A,C,E, showing firing rate breakdown by: cue type (top PETH), cue identity (top-middle PETH), cue location (bottom-middle PETH), and cue outcome (bottom PETH).

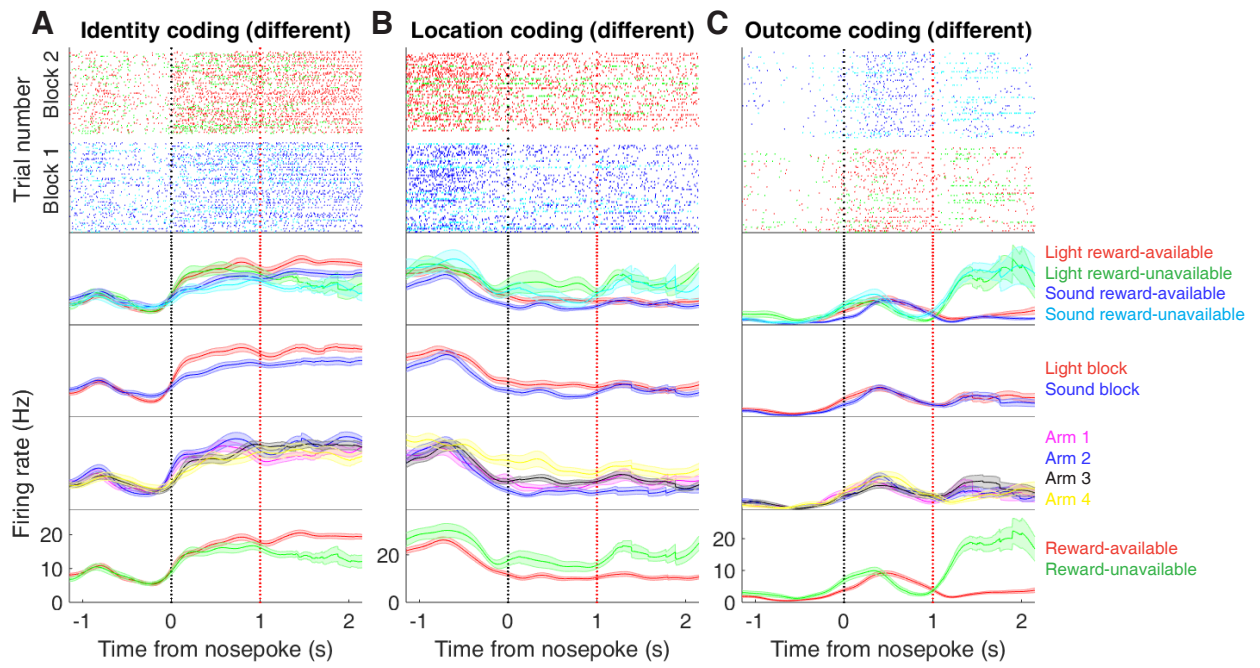


Figure 6 supplement 2: Expanded examples of cue-modulated NAc units influenced by different cue features at time of nosepoke for Figure 6B,D,F, showing firing rate breakdown by: cue type (top PETH), cue identity (top-middle PETH), cue location (bottom-middle PETH), and cue outcome (bottom PETH).

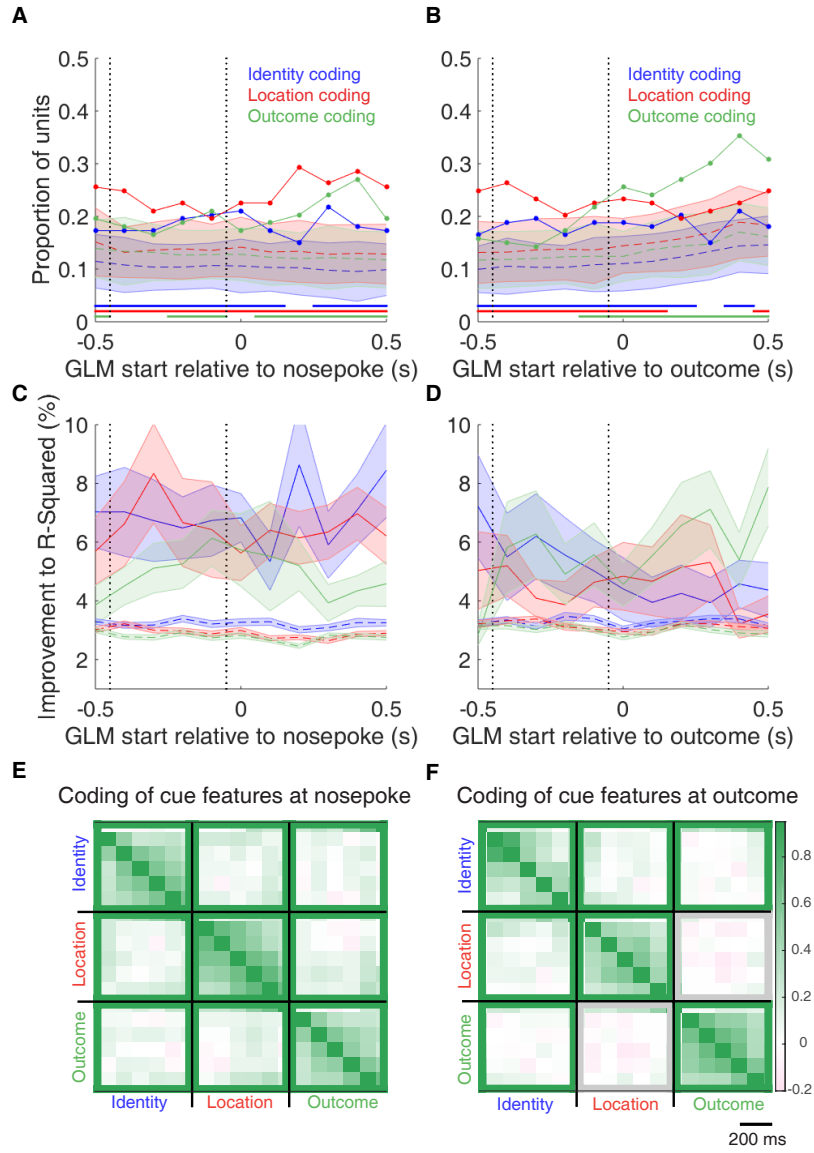


Figure 7 supplement 1: Summary of influence of cue features on cue-modulated NAc units at time points surrounding nosepoke and subsequent receipt of outcome. **A-B:** Sliding window GLM illustrating the proportion of cue-modulated units influenced by various predictors around time of nosepoke (A), and outcome (B). **A:** Sliding window GLM (bin size: 500 ms; step size: 100 ms) demonstrating the proportion of cue-modulated units where cue identity (blue solid line), location (red solid line), and outcome (green solid line) significantly contributed to the model at various time epochs relative to when the rat made a nosepoke. Dashed colored lines indicate the average of shuffling the firing rate order that went into the GLM 100 times. Error bars indicate 1.96 standard deviations from the shuffled mean. Solid lines at the bottom indicate when the proportion of units observed was greater than the shuffled distribution ($z\text{-score} > 1.96$). Points in between the two vertical dashed lines indicate bins where both pre- and post-cue-onset time periods were used in the GLM. **B:** Same as A, but for time epochs relative to receipt of outcome after the rat got feedback about his approach. **C-D:** Average improvement to model fit. **C:** Average percent improvement to R^2 for units where cue identity (blue solid line), location (red solid line), or outcome (green solid line) were significant contributors to the final model for time epochs relative to nosepoke. Dashed colored lines indicate the average of shuffling the firing rate order that went into the GLM 100 times. Shaded area around mean represents the standard error of the mean. **D:** Same C, but for time epochs relative to receipt of outcome. **E-F:** Correlation matrices testing the presence and overlap of cue feature coding at nosepoke (E) and outcome (F). **E:** Correlation matrix showing the correlation among identity, location, and outcome coding at nosepoke. Each of the 9 blocks represents correlations for two cue features across various nosepoke-centered time bins from the sliding window GLM, with green representing positive correlations ($r > 0$), pink negative correlations ($r < 0$), and grey representing no significant correlation ($r = 0$). X- and y-axis have the same axis labels, therefore the diagonal represents the correlation of a cue feature against itself at that particular time point ($r = 1$). The window of GLMs used in each block is from the onset of the task phase to the 500 ms window post-onset, in 100 ms steps. Each individual value is for a sliding window GLM within that range, with the scale bar contextualizing step size. Colored square borders around each block indicate the result of a comparison of the mean correlation to a shuffled distribution, with pink indicating separate populations ($z\text{-score} < -1.96$), grey indicating overlapping but independent populations, and green indicating joint overlapping populations ($z\text{-score} > 1.96$). **F:** Same as E, but for time bins following outcome receipt. Color bar displays relationship between correlation value and color.

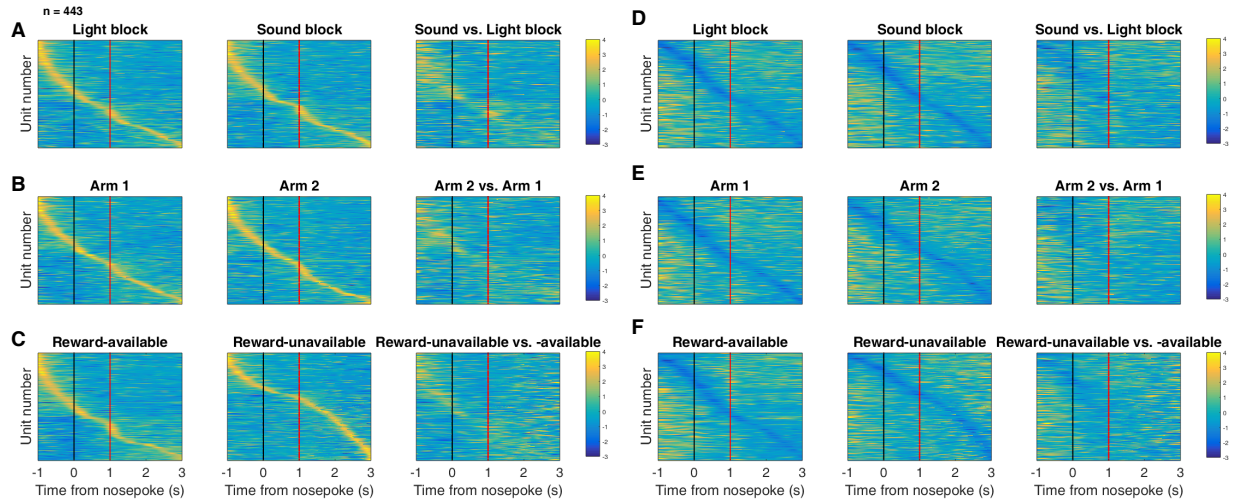


Figure 7 supplement 2: Distribution of NAc firing rates across time surrounding nosepoke for approach trials. Each panel shows normalized (z-score) firing rates for all recorded NAc units (each row corresponds to one unit) as a function of time (time 0 indicates nosepoke), averaged across all approach trials for a specific cue type, indicated by text labels. **A-C:** Heat plots aligned to normalized peak firing rates. **A, far left:** Heat plot showing smoothed normalized firing activity of all recorded NAc units ordered according to the time of their peak firing rate during the light block. Each row is a units average activity across time to the light block. Black dashed line indicates nosepoke. Red dashed line indicates reward delivery occurring 1 s after nosepoke for reward-available trials. Notice the yellow band across time, indicating all aspects of visualized task space were captured by the peak firing rates of various units. **A, middle:** Same units ordered according to the time of the peak firing rate during the sound block. Note that for both blocks, units tile time approximately uniformly with a clear diagonal of elevated firing rates, and a clustering around outcome receipt. **A, right:** Unit firing rates taken from the sound block, ordered according to peak firing rate taken from the light block. Note that a weaker but still discernible diagonal persists, indicating partial similarity between firing rates in the two blocks. Color bar displays relationship between z-score and color. **B:** Same layout as in A, except that the panels now compare two different locations on the track instead of two cue modalities. As for the different cue modalities, NAc units clearly discriminate between locations, but also maintain some similarity across locations, as evident from the visible diagonal in the right panel. Two example locations were used for display purposes; other location pairs showed a similar pattern. **C:** Same layout as in A, except that panels now compare correct reward-available and incorrect reward-unavailable trials. The disproportionate coding around outcome receipt for reward-available, but not reward-unavailable trials suggests encoding of reward receipt by NAc units. **D-F:** Heat plots aligned to normalized minimum firing rates. **D:** Responses during different stimulus blocks as in A, but with units ordered according to the time of their minimum firing rate. **E:** Responses during trials on different arms as in B, but with units ordered by their minimum firing rate. **F:** Responses during cues signaling different outcomes as in C, but with units ordered by their minimum firing rate. Overall, NAc units coded experience on the task, as opposed to being confined to specific task events only. Units from all sessions and animals were pooled for this analysis.

510 **References**

- 511 Akaishi, R., Kolling, N., Brown, J. W., & Rushworth, M. (2016). Neural Mechanisms of Credit Assignment in a Multicue
512 Environment. *Journal of Neuroscience*, 36(4), 1096–1112. doi: 10.1523/JNEUROSCI.3159-15.2016
- 513 Ambroggi, F., Ishikawa, A., Fields, H. L., & Nicola, S. M. (2008). Basolateral Amygdala Neurons Facilitate Reward-Seeking
514 Behavior by Exciting Nucleus Accumbens Neurons. *Neuron*, 59(4), 648–661. doi: 10.1016/j.neuron.2008.07.004
- 515 Asaad, W. F., Lauro, P. M., Perge, J. A., & Eskandar, E. N. (2017). Prefrontal Neurons Encode a Solution to the Credit-Assignment
516 Problem. *The Journal of Neuroscience*, 37(29), 6995–7007. doi: 10.1523/JNEUROSCI.3311-16.2017
- 517 Atallah, H. E., McCool, A. D., Howe, M. W., & Graybiel, A. M. (2014). Neurons in the ventral striatum exhibit cell-type-specific
518 representations of outcome during learning. *Neuron*, 82(5), 1145–1156. doi: 10.1016/j.neuron.2014.04.021
- 519 Averbeck, B. B., & Costa, V. D. (2017). Motivational neural circuits underlying reinforcement learning. *Nature Neuroscience*,
520 20(4), 505–512. doi: 10.1038/nn.4506
- 521 Barnes, T. D., Kubota, Y., Hu, D., Jin, D. Z., & Graybiel, A. M. (2005). Activity of striatal neurons reflects dynamic encoding and
522 recoding of procedural memories. *Nature*, 437(7062), 1158–1161. doi: 10.1038/nature04053
- 523 Bartra, O., McGuire, J. T., & Kable, J. W. (2013). The valuation system: A coordinate-based meta-analysis
524 of BOLD fMRI experiments examining neural correlates of subjective value. *NeuroImage*, 76, 412–427. doi:
525 10.1016/J.NEUROIMAGE.2013.02.063
- 526 Berke, J. D., Breck, J. T., & Eichenbaum, H. (2009). Striatal Versus Hippocampal Representations During Win-Stay Maze Perform-
527 ance. *Journal of Neurophysiology*, 101(3), 1575–1587. doi: 10.1152/jn.91106.2008
- 528 Berridge, K. C. (2012). From prediction error to incentive salience: Mesolimbic computation of reward motivation. *European
529 Journal of Neuroscience*, 35(7), 1124–1143. doi: 10.1111/j.1460-9568.2012.07990.x
- 530 Bissonette, G. B., Burton, A. C., Gentry, R. N., Goldstein, B. L., Hearn, T. N., Barnett, B. R., ... Roesch, M. R. (2013). Separate
531 Populations of Neurons in Ventral Striatum Encode Value and Motivation. *PLoS ONE*, 8(5), e64673. doi: 10.1371/jour-
532 nal.pone.0064673
- 533 Bouton, M. E. (1993). Context, time, and memory retrieval in the interference paradigms of Pavlovian learning. *Psychological
534 Bulletin*, 114(1), 80–99. doi: 10.1371/journal.pone.0064673
- 535 Carelli, R. M. (2010). Drug Addiction: Behavioral Neurophysiology. In *Encyclopedia of neuroscience* (pp. 677–682). Elsevier.
536 doi: 10.1016/B978-008045046-9.01546-1
- 537 Chang, S. E., & Holland, P. C. (2013). Effects of nucleus accumbens core and shell lesions on autosshaped lever-pressing. *Be-
538 havioural Brain Research*, 256, 36–42. doi: 10.1016/j.bbr.2013.07.046
- 539 Chang, S. E., Wheeler, D. S., & Holland, P. C. (2012). Roles of nucleus accumbens and basolateral amygdala in autosshaped lever
540 pressing. *Neurobiology of Learning and Memory*, 97(4), 441–451. doi: 10.1016/j.nlm.2012.03.008

- 541 Chau, B. K. H., Sallet, J., Papageorgiou, G. K., Noonan, M. A. P., Bell, A. H., Walton, M. E., & Rushworth, M. F. S. (2015).
542 Contrasting Roles for Orbitofrontal Cortex and Amygdala in Credit Assignment and Learning in Macaques. *Neuron*, 87(5),
543 1106–1118. doi: 10.1016/j.neuron.2015.08.018
- 544 Cheer, J. F., Aragona, B. J., Heien, M. L. A. V., Seipel, A. T., Carelli, R. M., & Wightman, R. M. (2007). Coordinated
545 Accumbal Dopamine Release and Neural Activity Drive Goal-Directed Behavior. *Neuron*, 54(2), 237–244. doi:
546 10.1016/j.neuron.2007.03.021
- 547 Cohen, J. D., & Servan-Schreiber, D. (1992). Context, cortex, and dopamine: a connectionist approach to behavior and biology in
548 schizophrenia. *Psychological Review*, 99(1), 45.doi: 10.1016/j.neuron.2007.03.021
- 549 Cooch, N. K., Stalnaker, T. A., Wied, H. M., Bali-Chaudhary, S., McDannald, M. A., Liu, T. L., & Schoenbaum, G. (2015).
550 Orbitofrontal lesions eliminate signalling of biological significance in cue-responsive ventral striatal neurons. *Nature Com-
551 munications*, 6, 7195. doi: 10.1038/ncomms8195
- 552 Corbit, L. H., & Balleine, B. W. (2011). The General and Outcome-Specific Forms of Pavlovian-Instrumental Transfer Are
553 Differentially Mediated by the Nucleus Accumbens Core and Shell. *Journal of Neuroscience*, 31(33), 11786–11794. doi:
554 10.1523/JNEUROSCI.2711-11.2011
- 555 Corlett, P. R., Taylor, J. R., Wang, X.-J., Fletcher, P. C., & Krystal, J. H. (2010). Toward a neurobiology of delusions. *Progress in
556 Neurobiology*, 92, 345–369. doi: 10.1016/j.pneurobio.2010.06.007
- 557 Cromwell, H. C., & Schultz, W. (2003). Effects of Expectations for Different Reward Magnitudes on Neuronal Activity in Primate
558 Striatum. *Journal of Neurophysiology*, 89(5), 2823–2838. doi: 10.1152/jn.01014.2002
- 559 Day, J. J., Roitman, M. F., Wightman, R. M., & Carelli, R. M. (2007). Associative learning mediates dynamic shifts in dopamine
560 signaling in the nucleus accumbens. *Nature Neuroscience*, 10(8), 1020–1028. doi: 10.1038/nn1923
- 561 Day, J. J., Wheeler, R. A., Roitman, M. F., & Carelli, R. M. (2006). Nucleus accumbens neurons encode Pavlovian approach behav-
562 iors: Evidence from an autoshaping paradigm. *European Journal of Neuroscience*, 23(5), 1341–1351. doi: 10.1111/j.1460-
563 9568.2006.04654.x
- 564 Dejean, C., Sitko, M., Girardeau, P., Bennabi, A., Caillé, S., Cador, M., ... Le Moine, C. (2017). Memories of Opiate Withdrawal
565 Emotional States Correlate with Specific Gamma Oscillations in the Nucleus Accumbens. *Neuropsychopharmacology*,
566 42(5), 1157–1168. doi: 10.1038/npp.2016.272
- 567 du Hoffmann, J., & Nicola, S. M. (2014). Dopamine Invigorates Reward Seeking by Promoting Cue-Evoked Excitation in the
568 Nucleus Accumbens. *Journal of Neuroscience*, 34(43), 14349–14364. doi: 10.1523/JNEUROSCI.3492-14.2014
- 569 Estes, W. K. (1943). Discriminative conditioning. I. A discriminative property of conditioned anticipation. *Journal of Experimental
570 Psychology*, 32(2), 150–155. doi: 10.1037/h0058316
- 571 Fitzgerald, T. H. B., Schwartenbeck, P., & Dolan, R. J. (2014). Reward-Related Activity in Ventral Striatum Is Action Contingent
572 and Modulated by Behavioral Relevance. *Journal of Neuroscience*, 34(4), 1271–1279. doi: 10.1523/JNEUROSCI.4389-
573 13.2014

- 574 Flagel, S. B., Clark, J. J., Robinson, T. E., Mayo, L., Czuj, A., Willuhn, I., ... Akil, H. (2011). A selective role for dopamine in
575 stimulus-reward learning. *Nature*, 469(7328), 53–59. doi: 10.1038/nature09588
- 576 Floresco, S. B. (2015). The Nucleus Accumbens: An Interface Between Cognition, Emotion, and Action. *Annual Review of
577 Psychology*, 66(1), 25–52. doi: 10.1146/annurev-psych-010213-115159
- 578 Floresco, S. B., Ghods-Sharifi, S., Vexelman, C., & Magyar, O. (2006). Dissociable roles for the nucleus accumbens core and shell
579 in regulating set shifting. *Journal of Neuroscience*, 26(9), 2449–2457. doi: 10.1523/JNEUROSCI.4431-05.2006
- 580 Frank, M. J., Seeberger, L. C., & O'Reilly, R. C. (2004). By carrot or by stick: Cognitive reinforcement learning in Parkinsonism.
581 *Science*, 306(5703), 1940–1943. doi: 10.1126/science.1102941
- 582 Giertler, C., Bohn, I., & Hauber, W. (2004). Transient inactivation of the rat nucleus accumbens does not impair guidance of
583 instrumental behaviour by stimuli predicting reward magnitude. *Behavioural Pharmacology*, 15(1), 55–63. doi: 10.1126/sci-
584 ence.1102941
- 585 Goldstein, B. L., Barnett, B. R., Vasquez, G., Tobia, S. C., Kashtelyan, V., Burton, A. C., ... Roesch, M. R. (2012). Ventral Striatum
586 Encodes Past and Predicted Value Independent of Motor Contingencies. *Journal of Neuroscience*, 32(6), 2027–2036. doi:
587 10.1523/JNEUROSCI.5349-11.2012
- 588 Goto, Y., & Grace, A. A. (2008). Limbic and cortical information processing in the nucleus accumbens. *Trends in Neurosciences*,
589 31(11), 552–558. doi: 10.1016/j.tins.2008.08.002
- 590 Gradin, V. B., Kumar, P., Waiter, G., Ahearn, T., Stickle, C., Milders, M., ... Steele, J. D. (2011). Expected value and prediction
591 error abnormalities in depression and schizophrenia. *Brain*, 134(6), 1751–1764. doi: 10.1093/brain/awr059
- 592 Grant, D. A., & Berg, E. (1948). A behavioral analysis of degree of reinforcement and ease of shifting to new responses in a
593 Weigl-type card-sorting problem. *Journal of Experimental Psychology*, 38(4), 404–411. doi: 10.1037/h0059831
- 594 Hamid, A. A., Pettibone, J. R., Mabrouk, O. S., Hetrick, V. L., Schmidt, R., Vander Weele, C. M., ... Berke, J. D. (2015).
595 Mesolimbic dopamine signals the value of work. *Nature Neuroscience*, 19(1), 117–126. doi: 10.1038/nn.4173
- 596 Hart, A. S., Rutledge, R. B., Glimcher, P. W., & Phillips, P. E. M. (2014). Phasic Dopamine Release in the Rat Nucleus Ac-
597 cumbens Symmetrically Encodes a Reward Prediction Error Term. *The Journal of Neuroscience*, 34(3), 698–704. doi:
598 10.1523/JNEUROSCI.2489-13.2014
- 599 Hassani, O. K., Cromwell, H. C., & Schultz, W. (2001). Influence of Expectation of Different Rewards on Behavior-Related
600 Neuronal Activity in the Striatum. *Journal of Neurophysiology*, 85(6), 2477–2489. doi: 10.1152/jn.2001.85.6.2477
- 601 Hearst, E., & Jenkins, H. M. (1974). *Sign-tracking: the stimulus-reinforcer relation and directed action*. Psychonomic Society. doi:
602 10.1152/jn.2001.85.6.2477
- 603 Hill, D. N., Mehta, S. B., & Kleinfeld, D. (2011). Quality Metrics to Accompany Spike Sorting of Extracellular Signals. *Journal of
604 Neuroscience*, 31(24), 8699–8705. doi: 10.1523/JNEUROSCI.0971-11.2011
- 605 Holland, P. C. (1992). Occasion setting in pavlovian conditioning. *Psychology of Learning and Motivation*, 28(C), 69–125. doi:
606 10.1016/S0079-7421(08)60488-0

- 607 Hollerman, J. R., Tremblay, L., & Schultz, W. (1998). Influence of Reward Expectation on Behavior-Related Neuronal Activity in
608 Primate Striatum. *Journal of Neurophysiology*, 80(2), 947–963. doi: 10.1152/jn.1998.80.2.947
- 609 Honey, R. C., Iordanova, M. D., & Good, M. (2014). Associative structures in animal learning: Dissociating elemental and
610 configural processes. *Neurobiology of Learning and Memory*, 108, 96–103. doi: 10.1016/j.nlm.2013.06.002
- 611 Hyman, S. E., Malenka, R. C., & Nestler, E. J. (2006). NEURAL MECHANISMS OF ADDICTION: The Role of Reward-Related
612 Learning and Memory. *Annual Review of Neuroscience*, 29(1), 565–598. doi: 10.1146/annurev.neuro.29.051605.113009
- 613 Ikemoto, S. (2007). Dopamine reward circuitry: Two projection systems from the ventral midbrain to the nucleus accumbens-
614 olfactory tubercle complex. *Brain Research Reviews*, 56(1), 27–78. doi: 10.1016/j.brainresrev.2007.05.004
- 615 Ishikawa, A., Ambroggi, F., Nicola, S. M., & Fields, H. L. (2008). Dorsomedial Prefrontal Cortex Contribution to Behav-
616 ioral and Nucleus Accumbens Neuronal Responses to Incentive Cues. *Journal of Neuroscience*, 28(19), 5088–5098. doi:
617 10.1523/JNEUROSCI.0253-08.2008
- 618 Joel, D., Niv, Y., & Ruppin, E. (2002). Actor-critic models of the basal ganglia: new anatomical and computational perspectives.
619 *Neural Networks*, 15(4-6), 535–547. doi: 10.1016/S0893-6080(02)00047-3
- 620 Kaczkurkin, A. N., Burton, P. C., Chazin, S. M., Manbeck, A. B., Espensen-Sturges, T., Cooper, S. E., ... Lissek, S. (2017).
621 Neural substrates of overgeneralized conditioned fear in PTSD. *American Journal of Psychiatry*, 174(2), 125–134. doi:
622 10.1176/appi.ajp.2016.15121549
- 623 Kaczkurkin, A. N., & Lissek, S. (2013). Generalization of Conditioned Fear and Obsessive-Compulsive Traits. *Journal of Psychol-
624 ogy & Psychotherapy*, 7, 3. doi: 10.4172/2161-0487.S7-003
- 625 Kalivas, P. W., & Volkow, N. D. (2005). The neural basis of addiction: A pathology of motivation and choice. *American Journal of
626 Psychiatry*, 162(8), 1403–1413. doi: 10.1176/appi.ajp.162.8.1403
- 627 Kapur, S. (2003). Psychosis as a state of aberrant salience: A framework linking biology, phenomenology, and pharmacology in
628 schizophrenia. *American Journal of Psychiatry*, 160(1), 13–23. doi: 10.1176/appi.ajp.160.1.13
- 629 Khamassi, M., & Humphries, M. D. (2012). Integrating cortico-limbic-basal ganglia architectures for learning model-based and
630 model-free navigation strategies. *Frontiers in Behavioral Neuroscience*, 6, 79. doi: 10.3389/fnbeh.2012.00079
- 631 Khamassi, M., Mulder, A. B., Tabuchi, E., Douchamps, V., & Wiener, S. I. (2008). Anticipatory reward signals in ventral striatal
632 neurons of behaving rats. *European Journal of Neuroscience*, 28(9), 1849–1866. doi: 10.1111/j.1460-9568.2008.06480.x
- 633 Lansink, C. S., Goltstein, P. M., Lankelma, J. V., Joosten, R. N. J. M. A., McNaughton, B. L., & Pennartz, C. M. A. (2008).
634 Preferential Reactivation of Motivationally Relevant Information in the Ventral Striatum. *Journal of Neuroscience*, 28(25),
635 6372–6382. doi: 10.1523/JNEUROSCI.1054-08.2008
- 636 Lansink, C. S., Goltstein, P. M., Lankelma, J. V., McNaughton, B. L., & Pennartz, C. M. (2009). Hippocampus leads ventral
637 striatum in replay of place-reward information. *PLoS Biology*, 7(8), e1000173. doi: 10.1371/journal.pbio.1000173
- 638 Lansink, C. S., Jackson, J. C., Lankelma, J. V., Ito, R., Robbins, T. W., Everitt, B. J., & Pennartz, C. M. A. (2012). Reward Cues
639 in Space: Commonalities and Differences in Neural Coding by Hippocampal and Ventral Striatal Ensembles. *Journal of*

- 640 *Neuroscience*, 32(36), 12444–12459. doi: 10.1523/JNEUROSCI.0593-12.2012
- 641 Lansink, C. S., Meijer, G. T., Lankelma, J. V., Vinck, M. A., Jackson, J. C., & Pennartz, C. M. A. (2016). Reward Expectancy
642 Strengthens CA1 Theta and Beta Band Synchronization and Hippocampal-Ventral Striatal Coupling. *Journal of Neuro-*
643 *science*, 36(41), 10598–10610. doi: 10.1523/JNEUROSCI.0682-16.2016
- 644 Lavoie, A. M., & Mizumori, S. J. (1994). Spatial, movement- and reward-sensitive discharge by medial ventral striatum neurons of
645 rats. *Brain Research*, 638(1-2), 157–168. doi: 10.1016/0006-8993(94)90645-9
- 646 Lee, D., Seo, H., & Jung, M. W. (2012). Neural Basis of Reinforcement Learning and Decision Making. *Annual Review of*
647 *Neuroscience*, 35(1), 287–308. doi: 10.1146/annurev-neuro-062111-150512
- 648 Levy, D. J., & Glimcher, P. W. (2012). The root of all value: a neural common currency for choice. *Current Opinion in Neurobiology*,
649 22, 1027–1038. doi: 10.1016/j.conb.2012.06.001
- 650 Lissek, S., Kaczkurkin, A. N., Rabin, S., Geraci, M., Pine, D. S., & Grillon, C. (2014). Generalized anxiety disor-
651 der is associated with overgeneralization of classically conditioned fear. *Biological Psychiatry*, 75(11), 909–915. doi:
652 10.1016/j.biopsych.2013.07.025
- 653 Logothetis, N. K., Pauls, J., Augath, M., Trinath, T., & Oeltermann, A. (2001). Neurophysiological investigation of the basis of the
654 fMRI signal. *Nature*, 412(6843), 150–157. doi: 10.1038/35084005
- 655 Maia, T. V. (2009). Reinforcement learning, conditioning, and the brain: Successes and challenges. *Cognitive, Affective and*
656 *Behavioral Neuroscience*, 9(4), 343–364. doi: 10.3758/CABN.9.4.343
- 657 Maia, T. V., & Frank, M. J. (2011). From reinforcement learning models to psychiatric and neurological disorders. *Nature*
658 *Neuroscience*, 14(2), 154–162. doi: 10.1038/nn.2723
- 659 Malhotra, S., Cross, R. W., Zhang, A., & Van Der Meer, M. A. A. (2015). Ventral striatal gamma oscillations are highly variable
660 from trial to trial, and are dominated by behavioural state, and only weakly influenced by outcome value. *European Journal*
661 *of Neuroscience*, 42(10), 2818–2832. doi: 10.1038/nn.2723
- 662 McDannald, M. A., Lucantonio, F., Burke, K. A., Niv, Y., & Schoenbaum, G. (2011). Ventral Striatum and Orbitofrontal Cortex
663 Are Both Required for Model-Based, But Not Model-Free, Reinforcement Learning. *Journal of Neuroscience*, 31(7), 2700–
664 2705. doi: 10.1523/JNEUROSCI.5499-10.2011
- 665 McGinty, V. B., Lardeux, S., Taha, S. A., Kim, J. J., & Nicola, S. M. (2013). Invigoration of reward seeking by cue and proximity
666 encoding in the nucleus accumbens. *Neuron*, 78(5), 910–922. doi: 10.1016/j.neuron.2013.04.010
- 667 Mulder, A. B., Shibata, R., Trullier, O., & Wiener, S. I. (2005). Spatially selective reward site responses in tonically active neurons
668 of the nucleus accumbens in behaving rats. *Experimental Brain Research*, 163(1), 32–43. doi: 10.1007/s00221-004-2135-3
- 669 Mulder, A. B., Tabuchi, E., & Wiener, S. I. (2004). Neurons in hippocampal afferent zones of rat striatum parse routes into
670 multi-pace segments during maze navigation. *European Journal of Neuroscience*, 19(7), 1923–1932. doi: 10.1111/j.1460-
671 9568.2004.03301.x
- 672 Nicola, S. M. (2004). Cue-Evoked Firing of Nucleus Accumbens Neurons Encodes Motivational Significance During a Discrimi-

- 673 native Stimulus Task. *Journal of Neurophysiology*, 91(4), 1840–1865. doi: 10.1152/jn.00657.2003
- 674 Nicola, S. M. (2010). The Flexible Approach Hypothesis: Unification of Effort and Cue-Responding Hypotheses for the Role of
675 Nucleus Accumbens Dopamine in the Activation of Reward-Seeking Behavior. *Journal of Neuroscience*, 30(49), 16585–
676 16600. doi: 10.1523/JNEUROSCI.3958-10.2010
- 677 Niv, Y., Daw, N. D., Joel, D., & Dayan, P. (2007). Tonic dopamine: Opportunity costs and the control of response vigor. *Psy-
678 chopharmacology*, 191(3), 507–520. doi: 10.1007/s00213-006-0502-4
- 679 Noonan, M. P., Chau, B. K., Rushworth, M. F., & Fellows, L. K. (2017). Contrasting Effects of Medial and Lateral Orbitofrontal
680 Cortex Lesions on Credit Assignment and Decision-Making in Humans. *The Journal of Neuroscience*, 37(29), 7023–7035.
681 doi: 10.1523/JNEUROSCI.0692-17.2017
- 682 Paxinos, G., & Watson, C. (1998). *The Rat Brain in Stereotaxic Coordinates* (4th ed.). San Diego: Academic Press. doi:
683 10.1523/JNEUROSCI.0692-17.2017
- 684 Pennartz, C. M. A. (2004). The Ventral Striatum in Off-Line Processing: Ensemble Reactivation during Sleep and Modulation by
685 Hippocampal Ripples. *Journal of Neuroscience*, 24(29), 6446–6456. doi: 10.1523/JNEUROSCI.0575-04.2004
- 686 Pennartz, C. M. A., Ito, R., Verschure, P., Battaglia, F., & Robbins, T. (2011). The hippocampalstriatal axis in learning, prediction
687 and goal-directed behavior. *Trends in Neurosciences*, 34(10), 548–559. doi: 10.1016/j.tins.2011.08.001
- 688 Peters, J., & Büchel, C. (2009). Overlapping and distinct neural systems code for subjective value during intertemporal and risky
689 decision making. *The Journal of neuroscience : the official journal of the Society for Neuroscience*, 29(50), 15727–34. doi:
690 10.1523/JNEUROSCI.3489-09.2009
- 691 Rescorla, R. A., & Solomon, R. L. (1967). Two-Process Learning Theory: Relationships Between Pavlovian Conditioning and
692 Instrumental Learning. *Psychological Review*, 74(3), 151–182. doi: 10.1037/h0024475
- 693 Robinson, T. E., & Flagel, S. B. (2009). Dissociating the Predictive and Incentive Motivational Properties of Reward-Related Cues
694 Through the Study of Individual Differences. *Biological Psychiatry*, 65(10), 869–873. doi: 10.1016/j.biopsych.2008.09.006
- 695 Roesch, M. R., Singh, T., Brown, P. L., Mullins, S. E., & Schoenbaum, G. (2009). Ventral Striatal Neurons Encode the Value
696 of the Chosen Action in Rats Deciding between Differently Delayed or Sized Rewards. *Journal of Neuroscience*, 29(42),
697 13365–13376. doi: 10.1523/JNEUROSCI.2572-09.2009
- 698 Roitman, M. F., Wheeler, R. A., & Carelli, R. M. (2005). Nucleus accumbens neurons are innately tuned for reward-
699 ing and aversive taste stimuli, encode their predictors, and are linked to motor output. *Neuron*, 45(4), 587–597. doi:
700 10.1016/j.neuron.2004.12.055
- 701 Saddoris, M. P., Stamatakis, A., & Carelli, R. M. (2011). Neural correlates of Pavlovian-to-instrumental transfer in the nucleus ac-
702 cumbens shell are selectively potentiated following cocaine self-administration. *European Journal of Neuroscience*, 33(12),
703 2274–2287. doi: 10.1111/j.1460-9568.2011.07683.x
- 704 Salamone, J. D., & Correa, M. (2012). The Mysterious Motivational Functions of Mesolimbic Dopamine. *Neuron*, 76(3), 470–485.
705 doi: 10.1016/j.neuron.2012.10.021

- 706 Schultz, W. (2016). Dopamine reward prediction error coding. *Dialogues in Clinical Neuroscience*, 18(1), 23–32. doi:
707 10.1038/nrn.2015.26
- 708 Schultz, W., Apicella, P., Scarnati, E., & Ljungberg, T. (1992). Neuronal activity in monkey ventral striatum related to the
709 expectation of reward. *The Journal of neuroscience : the official journal of the Society for Neuroscience*, 12(12), 4595–
710 610. doi: 10.1523/JNEUROSCI.12-12-04595.1992
- 711 Schultz, W., Dayan, P., & Montague, P. R. (1997). A neural substrate of prediction and reward. *Science*, 275(5306), 1593–1599.
712 doi: 10.1126/science.275.5306.1593
- 713 Sescousse, G., Li, Y., & Dreher, J.-C. (2015). A common currency for the computation of motivational values in the human striatum.
714 *Social Cognitive and Affective Neuroscience*, 10(4), 467–473. doi: 10.1093/scan/nsu074
- 715 Setlow, B., Schoenbaum, G., & Gallagher, M. (2003). Neural encoding in ventral striatum during olfactory discrimination learning.
716 *Neuron*, 38(4), 625–636. doi: 10.1016/S0896-6273(03)00264-2
- 717 Shidara, M., Aigner, T. G., & Richmond, B. J. (1998). Neuronal signals in the monkey ventral striatum related to progress through
718 a predictable series of trials. *Journal of Neuroscience*, 18(7), 2613–25. doi: 10.1016/S0896-6273(03)00264-2
- 719 Sjulson, L., Peyrache, A., Cumpelik, A., Cassataro, D., & Buzsáki, G. (2017). Cocaine place conditioning strengthens location-
720 specific hippocampal inputs to the nucleus accumbens. *bioRxiv*, 1–10. doi: 10.1101/105890
- 721 Sleezer, B. J., Castagno, M. D., & Hayden, B. Y. (2016). Rule Encoding in Orbitofrontal Cortex and Striatum Guides Selection.
722 *Journal of Neuroscience*, 36(44), 11223–11237. doi: 10.1523/JNEUROSCI.1766-16.2016
- 723 Strait, C. E., Sleezer, B. J., Blanchard, T. C., Azab, H., Castagno, M. D., & Hayden, B. Y. (2016). Neuronal selectivity
724 for spatial positions of offers and choices in five reward regions. *Journal of Neurophysiology*, 115(3), 1098–1111. doi:
725 10.1152/jn.00325.2015
- 726 Sugam, J. A., Saddoris, M. P., & Carelli, R. M. (2014). Nucleus accumbens neurons track behavioral preferences and reward
727 outcomes during risky decision making. *Biological Psychiatry*, 75(10), 807–816. doi: 10.1016/j.biopsych.2013.09.010
- 728 Sutton, R., & Barto, A. (1998). *Reinforcement Learning: An Introduction* (Vol. 9) (No. 5). MIT Press, Cambridge, MA. doi:
729 10.1109/TNN.1998.712192
- 730 Tabuchi, E. T., Mulder, A. B., & Wiener, S. I. (2000). Position and behavioral modulation of synchronization of hippocam-
731 pal and accumbens neuronal discharges in freely moving rats. *Hippocampus*, 10(6), 717–728. doi: 10.1002/1098-
732 1063(2000)10:6;717::AID-HIPO1009;3.0.CO;2-3
- 733 Takahashi, Y. K., Langdon, A. J., Niv, Y., & Schoenbaum, G. (2016). Temporal Specificity of Reward Prediction Errors
734 Signaled by Putative Dopamine Neurons in Rat VTA Depends on Ventral Striatum. *Neuron*, 91(1), 182–193. doi:
735 10.1016/j.neuron.2016.05.015
- 736 Tingley, D., & Buzsáki, G. (2018). Transformation of a Spatial Map across the Hippocampal-Lateral Septal Circuit. *Neuron*, 98(6),
737 1229–1242.e5. doi: 10.1016/J.NEURON.2018.04.028
- 738 van der Meer, M. A. A., & Redish, A. D. (2011). Theta Phase Precession in Rat Ventral Striatum Links Place and Reward

- 739 Information. *Journal of Neuroscience*, 31(8), 2843–2854. doi: 10.1523/JNEUROSCI.4869-10.2011
- 740 West, E. A., & Carelli, R. M. (2016). Nucleus Accumbens Core and Shell Differentially Encode Reward-Associated Cues after
741 Reinforcer Devaluation. *Journal of Neuroscience*, 36(4), 1128–1139. doi: 10.1523/JNEUROSCI.2976-15.2016
- 742 Wiener, S. I., Shibata, R., Tabuchi, E., Trullier, O., Albertin, S. V., & Mulder, A. B. (2003). Spatial and behavioral correlates in
743 nucleus accumbens neurons in zones receiving hippocampal or prefrontal cortical inputs. *International Congress Series*,
744 1250(C), 275–292. doi: 10.1016/S0531-5131(03)00978-6
- 745 Yun, I. A., Wakabayashi, K. T., Fields, H. L., & Nicola, S. M. (2004). The Ventral Tegmental Area Is Required for the Behavioral
746 and Nucleus Accumbens Neuronal Firing Responses to Incentive Cues. *Journal of Neuroscience*, 24(12), 2923–2933. doi:
747 10.1523/JNEUROSCI.5282-03.2004